COMPLEX SYSTEM MODELING AND SIMULATION
ISSN 2096-9929 01/06 pp 169−190
Volume 3, Number 3, September 2023
DOI: 10.23919/CSMS.2023.0011

# Low-Carbon Routing Based on Improved Artificial Bee Colony Algorithm for Electric Trackless Rubber-Tyred Vehicles

Yinan Guo, Yao Huang, Shirong Ge*, Yizhe Zhang, Ersong Jiang, Bin Cheng, and Shengxiang Yang

**Abstract:** Trackless rubber-tyerd vehicles are the core equipment for auxiliary transportation in inclined-shaft coal mines, and the rationality of their routes plays the direct impact on operation safety and energy consumption. Rich studies have been done on scheduling rubber-tyerd vehicles driven by diesel oil, however, less works are for electric trackless rubber-tyred vehicles. Furthermore, energy consumption of vehicles gives no consideration on the impact of complex roadway and traffic rules on driving, especially the limited cruising ability of electric trackless rubber-tyred vehichles (TRVs). To address this issue, an energy consumption model of an electric trackless rubber-tyred vehicle is formulated, in which the effects from total mass, speed profiles, slope of roadways, and energy management mode are all considered. Following that, a low-carbon routing model of electric trackless rubber-tyred vehicles is built to minimize the total energy consumption under the constraint of vehicle avoidance, allowable load, and endurance power. As a problem-solver, an improved artificial bee colony algorithm is put forward. More especially, an adaptive neighborhood search is designed to guide employed bees to select appropriate operator in a specific space. In order to assign onlookers to some promising food sources reasonably, their selection probability is adaptively adjusted. For a stagnant food source, a knowledge-driven initialization is developed to generate a feasible substitute. The experimental results on four real-world instances indicate that improved artificial bee colony algorithm (IABC) outperforms other comparative algorithms and the special designs in its three phases effectively avoid premature convergence and speed up convergence.

**Key words:** electric trackless rubber-tyred vehicles; low-carbon; routing; artificial bee colony algorithm

## 1 Introduction

In the construction and production phases of a coal mine, a large amount of materials, such as sand, cement, bolt-mesh, and so on, need to be carried by auxiliary transportation system from the ground to specific place underground, especially the moving face. Trackless rubber-tyred vehicles (TRVs), as the commonly-used transport equipment, are widely applied in inclined-shaft coal mines due to good adaptability and high flexibility[1]. However, complex roadway network and road condition underground,

• Yinan Guo and Shirong Ge are with the School of Mechanical Electronic and Information Engineering, China University of Mining and Technology (Beijing), Beijing 100083, China, and also with the Inner Mongolia Research Institute, China University of Mining and Technology (Beijing), Ordos 017010, China. E-mail: nanfly@126.com; gesr@cumtb.edu.cn.
• Yao Huang, Yizhe Zhang, Ersong Jiang, and Bin Cheng are with the School of Mechanical Electronic and Information Engineering, China University of Mining and Technology (Beijing), Beijing 100083, China.
• Shengxiang Yang is with the Institute of Artificial Intelligence, School of Computer Science and Informatics, De Montfort University, Leicester, LE1 9BH, UK. E-mail: syang@dmu.ac.uk.
* To whom correspondence should be addressed.
※ This article was recommended by Associate Editor Rui Wang.
Manuscript received: 2023-03-01; revised: 2023-04-05; accepted: 2023-05-02

such as diverse slope and uneven surface, easily result in low efficiency and high carbon emission of TRVs, even traffic accidents[2, 3]. Thus, it is of extraordinary significance to develop high-efficiency, energy-saving, and safe routing technique for TRVs.

Until now, most of TRVs are driven by diesel oil, causing strong vibration, loud noise, and high-pollution exhaust emission. To address the issue, Yan et al.[4] introduced a kind of tubular sandwiched engine mount in TRVs, producing good vibration-reducing performance. Bao et al.[2] analyzed the dynamics of TRVs and summarized the characterizing parameters that influence driving stability. Liu et al.[5] investigated the diffusion properties of particulate matter emitted by TRVs via numerical simulations and field measurements, and then optimized ventilation rate to reduce the exhaust emissions. Du[6] designed an anti-collision device for TRVs, with the purpose of guaranteeing the safe and efficient underground auxiliary transportation. Though the above techniques provide the obvious improvement on the driving performance of TRVs, the inherent drawbacks caused by diesel oil based power supply can not be overcome fully. With the development of electrically-driven technique, electric trackless rubber-tyred vehicles (ETRVs) have the advantages of light vibration, low noise, and zero exhaust, becoming a promising problem-solver for low-carbon production[7−9].

Except for power supply of TRVs, the inefficient routing is another factor that may result in high energy consumption, large loss of transportation capacity, and long waiting time, even safety accidents. To improve routing efficiency, Cai[10] constructed a TRV information system for underground transportation and gave the driving rules. Similarly, Han[11] introduced the intelligent dispatching system for TRVs, in which the precise positioning method and the regulation of underground traffic were given. In the above-mentioned systems, an efficient platform of high-speed information interaction is provided for TRVs, however, the global routing of TRVs that is mainly done in manual mode can obtain the satisfied but suboptimal dispatching scheme. To automatically generate a routing scheme, Zhou et al.[12] regarded the minimum driving distance as an objective and then formulated its mathematic model with the capacity constraint. Genetic algorithm was adopted as a problem-solver. However, the model is too simple to fully describe the necessary limitation and regulation of auxiliary transportation in practical scenario. In a roadway network underground, roads may have various slopes, which cannot be accurately reflected by Euclidean-based driving distance. Being different from it, energy consumption of TRVs has a direct relationship with road condition and driving mode, thus providing more reliable indicator for evaluating a routing scheme. In addition, except for the capacity, power supply of TRVs is also limited. More especially, ETRVs cannot be charged underground because all charging stations are located in pitheads. It is also noted that vehicles passing over each other is risky and even forbidden due to poor vision and narrow roads. The specific limitations of vehicle avoidance and explosion-proof charging make it much harder to achieve the optimal routing for ETRVs.

This issue is essentially the specific electric vehicle routing problem (EVRP). Rich studies have been done on finding the optimal routing scheme for conventional EVRP. CPLEX[13, 14], liner programming[15], and branch-and-price algorithm[16], as exact optimization techniques, can obtain satisfied but local optimal solution. With the development of intelligence optimization methods, variable neighborhood search[17], genetic algorithm[18], ant colony optimization[19], and artificial bee colony algorithm (ABC)[20] have been employed to achieve the optimal routing scheme within acceptable computational time. Among them, artificial bee colony algorithm inspired by bee colony behavior has simpler structure with few parameters and thus has been widely applied in solving combinatorial optimization problems, such as traveling salesman problem[21], arc routing problem[22], and vehicle routing problem[23, 24]. Although many problem-specific operators have been designed to enhance the ability of exploration and exploitation for ABC, their limitations will be exposed on solving other problems due to no free lunch theorems[25].

To address the above issues, low-carbon routing problem of ETRVs (LRPETRV) is formulated, in which the total energy consumption of ETRVs is taken as the optimized objective and the constraints of load capacity, cruising ability, and vehicle avoidance are considered. Following that, an improved ABC with three effective strategies is proposed for solving LRPETRV, with the purpose of speeding up convergence and enhancing solving accuracy. The main contributions of this paper are summarized as follows.

(1) To formulate a realistic mathematical model of the LRPETRV, the objective function is obtained via the energy consumption estimation considering road slope, vehicle load, and driving state, and the limitations from load capacity, cruising ability, and vehicle avoidance are taken into account.

(2) To solve LRPETRV efficiently, a strategy of adaptive neighborhood search is developed in employed bee phase to select suitable operator by evaluating their contribution to evolution, the onlooker phase adopts the adaptive selection probability considering both the quality and evolution efficiency of solutions to avoid the waste of computational cost, and a knowledge driving initialization strategy is proposed in scout phase to overstep the local extremum and improve convergence efficiency.

The remainder of this paper is organized as follows. Section 2 introduces various variants of EVRP and the optimization methods. Section 3 describes the LRPETRV in detail and presents its mathematical model. Section 4 describes the detail of the proposed improved artificial bee colony algorithm (IABC) for solving LRPETRV. The experimental studies are given in Section 5. Section 6 draws conclusions and provides the future research direction.

## 2 Related Work

This section provides a comprehensive discussion of previous work on TRV routing problem and EVRP, as well as studies on artificial bee colony algorithms that are typical problem-solvers for VRPs.

Trackless rubber-tyred vehicles are the core equipment of auxiliary transportation system in an inclined-shaft coal mine. The rationality of their routing plays a direct impact on the total transportation efficiency. Rich studies have been done on TRVs routing optimization. Zhang[26] designed a TRV dispatching platform to find an optimal route with the shortest distance, with the purpose of reducing resource waste. Considering poor vision and narrow roads, Zhou et al.[12] took the shortest path and the least number of meeting vehicles as optimization objectives and then built the mathematic model of TRVs routing problem. However, the above models give no consideration to the impact of complex road condition and traffic rules on TRV driving. In a roadway network with various slopes, Euclidean-based driving distance cannot effectively evaluate a routing scheme. Moreover, vehicles passing over each other may have a collision and even be forbidden in a narrow roadway. More especially, scheduling ETRVs meets the extra constraint due to the explosion-proof requirement and power limitation. But there is a lack of the related investigation on routing problem for ETRVs.

Low-carbon routing problem of ETRVs is essentially an electrical vehicle routing problem (EVRP) in a specific scenario. With the increasing application of electric vehicles, EVRP has been drawing much attention, and many valuable works have been put forward to find the optimal driving route under various objectives and constraints. The commonly-used optimizations objectives contain transportation time, energy consumption, and traveling distance and cost[27]. The constraints are normally derived from time, capacity, and power limitation. Ferro et al.[28] focused on time-of-use energy prices and took energy and distances cost as the optimization objective for EVRP. For EVRP with multi-depots, time windows, and nonlinear charging time, Karakatič[29] optimized the order of visiting service nodes and charging station, as well as charge time, with the purpose of minimizing the total transportation time that is the sum of driving time, waiting time, and recharging time. Considering the effects of environmental factors on energy consumption, Yi and Bauer[30] proposed a stochastic energy aware routing framework for electric vehicles with the goal of finding the optimal route having the minimum expectation of energy consumption. From low carbon perspective, Zhu et al.[31] formulated a multi-depot capacitated electric vehicle routing problem to a single-objective optimization, in which client demand is two-dimensional weighted items and the transportation distance is the objective. Under different recharging modes, EVRP with partial or full recharging[13, 32, 33] are investigated. Especially, the former has a significant flexibility with regard to recharging time. As we know, battery swap is a promising alternative to recharging battery due to its convenience and concurrent recharging mode. The battery can be recharged as electrical load is lower, cutting the cost[34]. Thus, the detours of taxi driving to battery swapping stations[35] were regarded as a new routing problem for electric vehicles. Taking the siting of recharging or battery swap station into account, bilevel optimization problem integrating site selection and routing is developed[36–38]. However, most of studies focused on EVRPs on the ground rather than underground, especially coal mines with narrow roadways and explosion-proof restriction.

No matter which kinds of EVRPs, energy consumption is an essential issue that has a direct impact on the route and its feasibility[39]. Generally, energy consumption of an electrical vehicle is calculated by linear deterministic functions. Almouhanna et al.[40] estimated energy consumption by scaling a consuming rate for a given distance. For an EVRP with load-dependent discharge and non-liner recharging, Kancharla and Ramadurai[41] formulated load-dependent discharging to a linear function with variable weight. Similarly, traveling distance, driving speed, load, and time are also be regarded as the variables in the liner functions for calculating energy consumption. However, they are too simple to accurately formulate energy consumption in complex transportation environment. To address the issue, Basso et al.[42] considered the speed profile and road topography and then formulated a non-linear function of energy consumption for EVRP. Perger and Auer[43] analyzed the influence of road topography, battery degradation, and additional loads on the total energy consumption and modeled them to a non-linear objective. Moreover, stochastic functions and machine learning have been introduced to calculate and predict energy consumption in different transportation instances[44−46]. Intuitively, non-liner deterministic functions or prediction methods may have higher requirements for computational cost and data. For an ETRV, the driving modes for roadways with various slopes may be different, which requires various power. In this case, a linear deterministic function cannot calculate the total energy consumption accurately. Thus, formulating a more precise model for energy consumption of a practical ETRV is necessary.

EVRP is a classical NP-hard problem, and it is impracticable to test all possible solutions due to the unaffordable computational cost and time[47]. Approximate methods are usually used as an effective problem-solver for EVRPs. For time-dependent EVRP with congestion tolls, Zhang et al.[48] proposed an allocating mechanism of recharging amounts and an adaptive large neighborhood search heuristic with an adjusting strategy of visit-beginning time. Considering both the uncertainty of customer demand and the weight-related energy consumption, Shen et al.[49] formulated a robust optimization model based on a route-related uncertain set and developed an adaptive large neighborhood search to solve it. Zhou et al.[13] presented a modified variable neighborhood search with a greedy algorithm to solve EVRP with partial recharge and vehicle recycling. This method can save cost effectively on real-world instances. Granada-Echeverri et al.[50] employed an iterated local search technique to solve EVRP with backhauls, and individuals are initialized by auxiliary graph based encoding to ensure their feasibility. Though neighborhood search based algorithms have achieved good performance on EVRP, their performance highly depends on the characteristics of a real-world routing problem. Moreover, the algorithm performance is sensitive to the quality of initial solution[19]. With the development of swam intelligent optimization algorithms and the wider application to combinatorial optimization, more and more studies introduced them to solve EVRPs. Zhu et al.[51] designed an improved neighbor routing method for EVRP with time window, and adaptive probability of crossover and mutation was introduced to elitist genetic algorithm, with the purpose of speeding up convergence. Zhang et al.[52] employed ant colony algorithm as problem-solver for EVRP and designed the benchmark instances for comparison of algorithm performance. Zhou and Tan[53] developed an improved discrete cuckoo search algorithm for solving a large-scale EVRP with the siting of battery swap stations. Although it has been proved that swarm intelligent optimization is a promising solver for EVRP, there lacks the studies on low-carbon routing problem of ETRVs. The exiting algorithms show a strong ability of exploration and exploitation for some specific problems, owing to their problem-specific operators, which has obvious limitations on addressing a new problem.

Inspired by foraging behavior of honeybee swarm, ABC was first proposed by Karaboga[54], in which three search phases, including employed bee, onlooker, and scout phase, are designed. With its wide application in knapsack problem[55−57], parameter optimization[58, 59], path planing[60−62], and machine scheduling[63, 64], it has been proved to be a promising solver for routing problems. Pandiri and Singh[65] developed a neighboring solution generation and improved scout phase of ABC to solve the colored traveling salesman problem effectively. Considering the different roles of employed bees and onlookers, Karaboga and Gorkemli[66] gave a new definition for the foraging behavior of onlookers and proposed quick ABC for solving the traveling salesman problem (TSP). For the reverse logistics location and routing problem, Guo and Zhang[67] proposed a discrete ABC with greedy adjustment strategy. Lei et al.[68] designed an

effective evaluation mechanism to dynamically determine employed bee and onlooker swarm, and then variable neighborhood descent was introduced in employed bee and onlooker phases. To solve the team orienteering problem, Trachanatzi et al.[69] presented a distance related ABC based on a novel encoding/decoding method. It is worth noting that the encoding scheme and the operators in three phases of ABC need to be specially designed for different routing problems, with the purpose of improving algorithm performance.

## 3 Description of Low-Carbon Routing Problem for ETRVs

For electric trackless rubber-tyred vehicles in a coal mines, finding their optimal routes to carry the materials from the ground to the destinations with minimum energy consumption under the limited capacity and power supply is essentially single-objective optimization problem with constraints. How to rationally evaluate energy consumption during the driving process and formulate the routing model is the basis of problem-solver.

### 3.1 Model formulation for low-carbon single-objective routing problem

To formulate the problem more rationally, some hypotheses are given in terms of the actual scenario. In a coal mine, all ETRVs start and end the transportation tasks at only one ground depot, in which sufficient charging stations locate. The charging time is negligible and the battery for each ETRV is full. No matter which kinds of materials, only their mass are considered. All materials are stored nearby the ground depot for loading, and their unloading time at each service node is fixed. The chambers for vehicle avoidance are located at the junction linking two sections of roadway.

Suppose that transportation tasks are distributed at $N$ service nodes underground, represented by $S=\{s_1, s_2,\ldots,s_i,\ldots,s_N\}$, and completed by $K$ homogeneous ETRVs with the same load $Q$ and battery capacity $B$. In each service node, the quantity of material that needs to be unloaded is known in advance and represented by $Q_{\mathrm{m}i}$, $i=1, 2, \ldots, N$, and its service time is ST. All service nodes and the ground depot compose of the nodes for a transportation network $G=(V,A)$, denoted as $V=\{s_0\}\cup S$. $A=\{(s_i,s_j)|s_i\in V, s_j\in V, i\neq j\}$ forms the arcs in $G$, and each arc $(s_i,s_j)$ corresponds to a path from $s_i$ to $s_j$. It is worthy noting that a path may contain more than one roadway. All roadways are connected via $M$ linking nodes, represented by $L=\{l_1,l_2,\ldots,l_p,\ldots,l_M\}$. A roadway between $l_p$ and $l_q$ is described by $r_{pq}, l_p\in L, l_q\in L, p\notin q$. Based on this, a path from $s_i$ to $s_j$ passing $m$ roadway is denoted as $(s_i,s_j)=\{s_i,\ldots,l_p,l_q,\ldots,s_j\}$. Assume that the driving time of a sub-path $r_{pq}$ is $t_{pq}$, $t_{ij}=\sum t_{pq}$ indicates the driving time of the path $(s_i,s_j)$. Taking the economic and environmental performances of trackless rubber-tyred vehicles underground into account, their low carbon routing problem can be formulated into the following single-objective constraint optimization one. Intuitively, an optimal routing scheme has the minimal total energy consumption.

$$\min F=\sum_{k=1}^{K}\sum_{i=0}^{N}\sum_{j=0}^{N}e_{ij}^{k}x_{ij}^{k} \tag{1}$$

where $e_{ij}^{k}$ is energy consumed by the $k$-th ETRV traveling the path $(s_i,s_j)$, which depends on the load, road condition, and driving speed. The detailed evaluation method is demonstrated in Section 3.2. $x_{ij}^{k}=1$ indicates the $k$-th ETRV drives from the service node $s_i$ to $s_j$ and performs their transportation tasks.

According to the operation regulation in coal mines and practical distribution of roadway networks, low-carbon routing of ETRVs must satisfy six constraints as follows.

**Constraint (1):** Two trackless rubber-tyred vehicles cannot pass through a roadway in the opposite direction at the same time.

$$T_{pq}^{k}\cap T_{qp}^{g}=\varnothing,\forall k,\ g\in\{1,2,\ldots,K\} \tag{2}$$

where $T_{pq}^{k}$ and $T_{qp}^{g}$ are the time intervals of the $k$-th and $g$-th ETRVs passing through $r_{pq}$, respectively.

**Constraint (2):** The total load brought by an ETRV must be within its maximum allowable one.

$$\sum_{i=1}^{N}Q_{\mathrm{m}i}x_{ij}^{k}<Q,\ \forall s_j\in V,\ k\in\{1,2,\ldots,K\} \tag{3}$$

**Constraint (3):** The battery capacity of an ETRV satisfies the need for completing its transportation task and returning to the ground depot.

$$\sum_{i=0}^{N}\sum_{j=0}^{N}e_{ij}^{k}x_{ij}^{k}<B,\ \forall i\neq j,\ k\in\{1,2,\ldots,K\} \tag{4}$$

**Constraint (4):** The time of ETRVs reaching or leaving a service node is feasible.

$$\tau_j^k\geqslant\tau_i^k+(t_{ij}+\mathrm{ST})x_{ij}^{k},\ \forall(s_i,s_j)\in A,\ k\in\{1,2,\ldots,K\} \tag{5}$$

$$\tau_q^k \geqslant \tau_p^k + t_{pq} x_{ij}^k,\ \forall l_p, l_q \in (s_i, s_j),\ k \in \{1,2,\ldots,K\} \quad (6)$$

where $\tau_i^k$ and $\tau_p^k$ represent the time of the $k$-th ETRV arriving at the $i$-th service node $s_i$ and the $p$-th linking node $l_p$, respectively.

**Constraint (5):** Each service node can only be visited once.

$$\sum_{k=1}^{K}\sum_{j=0}^{N} x_{ij}^k = 1,\ \forall s_j \in V \quad (7)$$

**Constraint (6):** The number of ETRVs reaching and leaving a service node must be the same.

$$\sum_{k=1}^{K}\sum_{i=0}^{N} x_{ij}^k = \sum_{k=1}^{K}\sum_{g=0}^{N} x_{jg}^k,\ \forall s_j \in V \quad (8)$$

### 3.2 Calculation of energy consumption for the ETRV

The energy consumption of an ETRV for completing a transportation task depends on its total mass, speed profiles, slope of roadways, and energy management mode[42]. Suppose that the length and slope of a roadway $r_{pq}$ are $d_{pq}$ and $\theta_{pq}$, respectively. ETRVs can pass through this roadway with the maximal allowable driving speed, represented by $v_{pq}$. For two roadways connecting each other, their direction, slope, pavement roughness, and speed limitation exist significant differences. Thus, an ETRV must slow down and pass through the linking node connecting the above two roadways with the low driving speed, denoted as $v_{\mathrm{L}}$, with the purpose of avoiding hitting the side wall of roadways.

Without loss of generality, an ETRV can drive by two speed levels in a roadway, namely $v_{pq}$ and $v_{\mathrm{L}}$. To speed up from $v_{\mathrm{L}}$ to $v_{pq}$, an ETRV adopts a fixed accelerated speed $a$, and vice versa. Thus, the driving mode of an ETRV can be partitioned into three phases, i.e., acceleration, steady-speed, and speed reduction. The corresponding energy consumption varies each other and is evaluated as follows.

In the accelerating phase, the speed of an ETRV increases over time.

$$v(t) = \begin{cases} at, & l_p \in \{l_0, s_i\}, i = 1,2,\ldots,N; \\ v_{\mathrm{L}} + at, & \text{else} \end{cases} \quad (9)$$

$$t_a = \frac{v_{pq} - v_{\mathrm{L}}}{a} \quad (10)$$

where $t_a$ is time-consumption in this phase. Denote $M_{pq}$ as the total mass of an ETRV when it passes $r_{pq}$, and the instantaneous mechanical power $P_{\mathrm{M}}(t)$ is calculated according to its longitudinal dynamics[70].

$$\begin{aligned} P_{\mathrm{M}}(t) = {} & aM_{pq}v(t) + M_{pq}gv(t)\sin\theta_{pq} + \\ & M_{pq}gv(t)C_{\mathrm{r}}\cos\theta_{pq} + 0.5C_{\mathrm{d}}F_{\mathrm{A}}\rho v(t)^3 \end{aligned} \quad (11)$$

where $g$ is the gravitational constant and $\rho$ is the air density. $C_{\mathrm{r}}$ and $C_{\mathrm{d}}$ are the rolling resistance coefficient and air drag coefficient, respectively. $F_{\mathrm{A}}$ represents the frontal area of an ETRV. By integrating $P_{\mathrm{M}}(t)$ in $t_a$, the mechanical energy $e_{\mathrm{M}_1}$ is obtained.

$$\begin{aligned} e_{\mathrm{M}_1} = {} & \frac{1}{3600}\int_0^{t_a} P_{\mathrm{M}}(t)\mathrm{d}t = \\ & \frac{1}{3600}\frac{v_{pq}^2 - v_{\mathrm{L}}^2}{2a} M_{pq}(a + g\sin\theta_{pq} + \\ & gC_{\mathrm{r}}\cos\theta_{pq} + 0.5C_{\mathrm{d}}F_{\mathrm{A}}\rho\frac{v_{pq}^2 + v_{\mathrm{L}}^2}{2M_{pq}}) \end{aligned} \quad (12)$$

It is worth noting that the powertrain is regenerating electric energy to battery as $e_{\mathrm{M}_1}$ is negative. Otherwise, the powertrain is in the mode of traction. Considering the electricity consumption of auxiliary devices and the energy loss in battery and powertrain, the total electric energy consumption in this phase is achieved as follows:

$$e_1 = \begin{cases} \dfrac{e_{\mathrm{M}_1}}{\eta_1\eta_2} + P_{\mathrm{A}}t_a, & e_{\mathrm{M}_1} \geqslant 0; \\ e_{\mathrm{M}_1}\eta_1\eta_2\eta_3 + P_{\mathrm{A}}t_a, & e_{\mathrm{M}_1} < 0 \end{cases} \quad (13)$$

where $\eta_1$, $\eta_2$, and $\eta_3$ are the efficiency for mechanical transmission, motor, and energy recovery, respectively. $P_{\mathrm{A}}$ represents the extra electrical power consumed by auxiliary devices.

Similarly, the mechanical energy $e_{\mathrm{M}_2}$ and electric energy consumption $e_2$ of the ETRV in steady-speed phase are calculated as follows:

$$\begin{aligned} e_{\mathrm{M}_2} = {} & \frac{1}{3600}(d_{pq} - \frac{v_{pq}^2 - v_{\mathrm{L}}^2}{a})(M_{pq}g\sin\theta_{pq} + \\ & M_{pq}gC_{\mathrm{r}}\cos\theta_{pq} + 0.5C_{\mathrm{d}}F_{\mathrm{A}}\rho v_{pq}^2) \end{aligned} \quad (14)$$

$$e_2 = \begin{cases} \dfrac{e_{\mathrm{M}_2}}{\eta_1\eta_2} + P_{\mathrm{A}}\dfrac{d_{pq}a - (v_{pq}^2 - v_{\mathrm{L}}^2)}{av_{pq}}, & e_{\mathrm{M}_2} \geqslant 0; \\ e_{\mathrm{M}_2}\eta_1\eta_2\eta_3 + P_{\mathrm{A}}\dfrac{d_{pq}a - (v_{pq}^2 - v_{\mathrm{L}}^2)}{av_{pq}}, & e_{\mathrm{M}_2} < 0 \end{cases} \quad (15)$$

The mechanical energy $e_{\mathrm{M}_3}$ and electric energy consumption $e_3$ of the ETRV in speed reduction phase are achieved.

$$\begin{aligned} e_{\mathrm{M}_3} = {} & \frac{1}{3600}\frac{v_{pq}^2 - v_{\mathrm{L}}^2}{2a} M_{pq}(-a + g\sin\theta_{pq} + \\ & gC_{\mathrm{r}}\cos\theta_{pq} + 0.5C_{\mathrm{d}}F_{\mathrm{A}}\rho\frac{v_{pq}^2 + v_{\mathrm{L}}^2}{2M_{pq}}) \end{aligned} \quad (16)$$

$$e_3=\begin{cases}\dfrac{e_{\mathrm{M}_3}}{\eta_1\eta_2}+P_{\mathrm{A}}\dfrac{v_{pq}-v_{\mathrm{L}}}{a}, & e_{\mathrm{M}_3}\geqslant 0;\\ e_{\mathrm{M}_3}\eta_1\eta_2\eta_3+P_{\mathrm{A}}\dfrac{v_{pq}-v_{\mathrm{L}}}{a}, & e_{\mathrm{M}_3}<0\end{cases}\tag{17}$$

Based on them, the electrical energy consumed by the $k$-th ETRV passing through $r_{pq}$ is the sum in all driving phases.

$$e_{pq}^k=e_1+e_2+e_3\tag{18}$$

For the $k$-th ETRV, its total electric energy consumption for driving from $s_i$ to $s_j$ is the cumulative sum of $e_{pq}^k$.

$$e_{ij}^k=\sum_{l_p,l_q\in(s_i,s_j)}e_{pq}^k x_{ij}^k\tag{19}$$

# 4 Improved ABC for Solving LRPETRV

To find the optimal feasible route for ETRVs, an improved artificial bee colony algorithm is put forward. As the pseudocode listed in Algorithm 1, a population is first initialized (Line 2). After evaluating the fitness value and calculating constraint violation of each individual (Lines 3 and 4), three phases of IABC, including adaptive neighborhood search, onlooker phase with adaptive selection probability, and knowledge-driven scout phase, are executed sequentially to update the population (Lines 7−9). First, an operator pool containing three kinds of neighborhood search operations is constructed, and the contribution of each operator is evaluated quantitatively by the performance improvement of offspring. Based on their historical and current contribution, an employed bee selects the most appropriate one by the roulette wheel to realize the effective local search. Second, adaptive selection probability is defined to evaluate each individual in terms of its performance and contribution to the evolution, with the purpose of improving the evolution efficiency. Third, a knowledge-driven initialization strategy is put forward to produce a new individual instead of the local optimum.

**Algorithm 1 Improved artificial bee colony algorithm**

**Input:** population size PS, the maximum termination iteration Maxgen, and the maximum number of invalid search $C^{\max}$

**Output:** The optimal feasible solution

1: gen = 0, $\varphi_o=1$, $C_i=0$;
2: Initialize a population $X$;
3: Evaluate $F(X_i)$;
4: Calculate $\mathrm{CV}_h(X_i)$ for all constraints;
5: **While** gen ⩽ Maxgen
6: gen ← gen + 1;
7: $(X,C_i,\varphi_o)\leftarrow$ EBP-ANS$(X,C_i,C^{\max},\varphi_o)$;
8: $(X,C_i)\leftarrow$ OP-ASP$(X,C_i,C^{\max})$;
9: $(X,C_i)\leftarrow$ KSP$(X,C_i,C^{\max})$;
10: **End while**
11: Return the optimal feasible solution in $X$

## 4.1 Encoding and decoding

A solution for LRPETRV is encoded by the integer vector, namely $X_i=\{0,\mathrm{sn}_1,\ldots,\mathrm{sn}_{j_1},0,\mathrm{sn}_{j_1+1},\ldots,\mathrm{sn}_{j_1+j_2},0,\ldots,0,\mathrm{sn}_{j_1+j_2+\cdots+j_{K-1}+1},\ldots,\mathrm{sn}_{j_1+j_2+\cdots+j_K},0\}$. The service nodes assigned to each ETRV are arranged in a specific service order and segmented with the ones for another ETRV by "0". The first and last "0" denotes the depot. Because all service nodes must be visited by at least one ETRV, $\sum_{k=1}^{K}j_k=N$. Thus, the length of an individual is $K$+$N$+1.

In order to conveniently evaluate the fitness value and constraint violation, an individual is decoded as follows. Taking an LRPETRV with 3 ETRVs, 10 service nodes, and 1 depot as an example, a solution represented by {0,6,3,7,0,8,5,1,2,0,4,9,10,0} is decoded to sub-routes for three ETRVs. They are $0\rightarrow6\rightarrow3\rightarrow7\rightarrow0$, $0\rightarrow8\rightarrow5\rightarrow1\rightarrow2\rightarrow0$, and $0\rightarrow4\rightarrow9\rightarrow10\rightarrow0$. More specifically, an ETRV leaves depot to complete the transportation tasks of the 6th, 3rd, and 7th service nodes in turn and return to depot finally.

## 4.2 Adaptive neighborhood search for employed bees

In the original ABC, employed bees seek better food sources by the specific neighborhood search strategy in terms of the fitness values. Though this operation contributes to the fast convergence, the solutions may fall into the infeasible search space due to the constraints of LRPETRV. To effectively exploit the feasible region, an adaptive neighborhood search (ANS) is put forward. Three kinds of neighborhood search operators are introduced to form a pool. Each operator is synthetically evaluated by fitness value and constraint violation of the generated solution. The one finding the best solutions has the highest probability to be adopted in the next iteration. This mechanism adaptively adjusts neighborhood search operators in terms of their contribution for a specific search space, improving the exploitation efficiency.

Define $\mathrm{Ns}=(\mathrm{Ns}_1,\mathrm{Ns}_2,\mathrm{Ns}_3)$ as a pool of common neighborhood search operators[71], and their details are

illustrated as follows.

- $\mathrm{Ns}_1$: Swapping operation is employed, in which two service nodes in $X_i$ are randomly selected and exchanged each other.
- $\mathrm{Ns}_2$: A section of an individual is selected, and all service nodes in this section are rearranged in a reverse order. We call this reversing operation.
- $\mathrm{Ns}_3$: A service node is relocated to another locus, termed as inserting operation.

Intuitively, each operator exploits its neighborhood with different granularity and intensity, thus, makes the offspring escaping from the infeasible search space, and improves its fitness to a various extent. To quantitatively evaluate the contribution of each operator on the evolution, a comprehensive score is defined to measure the improvement on fitness value and constraint violation.

$$\mathrm{Cs}_o = \mathrm{Cs}_o^{\mathrm{F}} + \mathrm{Cs}_o^{\mathrm{CV}},\ o = 1,2,3 \tag{20}$$

Let $X_i$ be an individual and $X_i^{\mathrm{new}}$ be its offspring generated by a selected neighborhood search operator. $\mathrm{Cs}_o^{\mathrm{F}}$ and $\mathrm{Cs}_o^{\mathrm{CV}}$ are evaluated by the degrees of improving fitness and meeting constraints between $X_i$ and $X_i^{\mathrm{new}}$, respectively. Apparently, the neighborhood search operator producing the offspring with better fitness value and smaller constraint violation is assigned the higher scores. For the selected operator, the sign function is employed to measure the improvement on fitness value and constraint violation between parents and offspring. It is worth noting that the comprehensive scores of unselected ones are not updated and keep their original values.

$$\mathrm{Cs}_o^{\mathrm{F}} = \mathrm{sgn}(F(X_i) - F(X_i^{\mathrm{new}})) \tag{21}$$

$$\mathrm{Cs}_o^{\mathrm{CV}} = \sum_{h=1}^{3} \mathrm{sgn}(\mathrm{CV}_h(X_i) - \mathrm{CV}_h(X_i^{\mathrm{new}})) \tag{22}$$

$$\begin{cases} \mathrm{CV}_1(X_i) = \sum\limits_{k=1}^{K-1} \sum\limits_{g=k+1}^{K} \max\{0, \sum\limits_{p=1}^{M} \sum\limits_{q=1,p\neq q}^{M} \mathrm{VM}_{pq}^{kg}\}, \\ \mathrm{CV}_2(X_i) = \sum\limits_{k=1}^{K} \max\{0, \sum\limits_{i=1}^{N} Q_{\mathrm{m}_i} x_{ij}^k - Q\}, \\ \mathrm{CV}_3(X_i) = \sum\limits_{k=1}^{K} \max\{0, \sum\limits_{i=0}^{N} \sum\limits_{j=0,i\neq j}^{N} e_{ij}^k x_{ij}^k - B\} \end{cases} \tag{23}$$

where $\mathrm{CV}_1(X_i)$, $\mathrm{CV}_2(X_i)$, and $\mathrm{CV}_3(X_i)$ represent the constraint violation of vehicle avoidance, allowable load, and endurance power, respectively. And $\mathrm{VM}_{pq}^{kg} = \begin{cases} 0, & T_{pq}^k \cap T_{qp}^g = \varnothing \\ 1, & \text{other} \end{cases}, \forall k, g \in \{1,2,\ldots,K\}$. Based on the above comprehensive score of each neighborhood search operator, its total contribution during the evolution is the sum of all historical scores, represented by $\varphi_o, o = 1,2,3$. Denote $w$ as the weight of the historical contribution, and the comprehensive score of each neighborhood search operator in current generation is emphasized by assigning a larger weight. According to Eqs. (21) and (22), $\mathrm{Cs}_o$ varies from −4 to 4. To facilitate calculating the selection probability in the roulette wheel method, total contribution is obtained as follows:

$$\varphi_o = \sum_{\mathrm{gen}-1} w\varphi_o^{\mathrm{gen}-1} + (1-w)(\mathrm{Cs}_o^{\mathrm{gen}} + 4) \tag{24}$$

Define the probability of selecting $\mathrm{Ns}_o$ as $\mathrm{Pn}_o$, and the roulette wheel selection is introduced to seek the most appropriate neighborhood search operator for an employed bee.

$$\mathrm{Pn}_o = \frac{\varphi_o}{\sum_{i=1}^{3} \varphi_i} \tag{25}$$

Then, the offspring $X_i^{\mathrm{new}}$ is generated by the selected neighborhood search operator on $X_i$. Only the offspring that is superior to its parent on fitness value or feasibility will be retained instead of $X_i$. That is,

$$X_i = \begin{cases} X_i, (F(X_i) \leqslant F(X_i^{\mathrm{new}}), \mathrm{CV}_h(X_i) = 0, \mathrm{CV}_h(X_i^{\mathrm{new}}) = 0, \\ \forall h) \cup \left( \sum\limits_{h=1}^{3} \mathrm{sgn}(\mathrm{CV}_h(X_i) - \mathrm{CV}_h(X_i^{\mathrm{new}})) \leqslant 0 \right); \\ X_i^{\mathrm{new}}, (F(X_i) > F(X_i^{\mathrm{new}}), \mathrm{CV}_h(X_i) = 0, \mathrm{CV}_h(X_i^{\mathrm{new}}) = 0, \\ \forall h) \cup \left( \sum\limits_{h=1}^{3} \mathrm{sgn}(\mathrm{CV}_h(X_i) - \mathrm{CV}_h(X_i^{\mathrm{new}})) > 0 \right) \end{cases} \tag{26}$$

The pseudocode of employed bee phase with ANS is shown in Algorithm 2.

### 4.3 Adaptive selection probability for onlooker

In onlooker phase, the individual selected by roulette wheel is exploited by local search strategy. The ones with better fitness values are assigned to higher selection probability and followed with more onlookers. However, too many onlookers fall into an infeasible search space, which may dedicate to the evolution to a lesser extent.

To improve the evolution efficiency, an adaptive selection probability is defined to evaluate each individual more rationally.

$$P_j = \frac{1}{4}\varepsilon_j \left( \frac{1 \Big/ F(X_j)}{\sum_{i=1}^{\mathrm{PS}} 1/F(X_i)} + \sum_{h=1}^{3} \frac{1 \Big/ (\mathrm{CV}_h(X_j) + \delta_h)}{\sum_{i=1}^{\mathrm{PS}} 1/(\mathrm{CV}_h(X_i) + \delta_h)} \right) \tag{27}$$

**Algorithm 2 Employed bee phase with ANS (EBP-ANS)**

**Input:** $X, \varphi_o, C_i, C^{\max}$

**Output:** $X, \varphi_o, C_i$

**For** $i = 1$ to PS
  **For** $o = 1$ to 3
    Calculate $\mathrm{Pn}_o$ by Eq. (25);
  **End for**
  Select an operator $\mathrm{Ns}_o$ by the roulette wheel selection in terms of $\mathrm{Pn}_o$;
  Produce $X_i^{\mathrm{new}}$ by $\mathrm{Ns}_o$ on $X_i$;
  Evaluate $F(X_i^{\mathrm{new}})$ and $\mathrm{CV}_h(X_i^{\mathrm{new}})$;
  Calculate $\mathrm{Cs}_o$ of $\mathrm{Ns}_o$;
  Update $\varphi_o$;
  Update $X_i$ by Eq. (26);
  **If** $X_i \leftarrow X_i^{\mathrm{new}}$
    $C_i \leftarrow 0$;
  **Else**
    $C_i \leftarrow C_i + 1$;
  **End if**
**End for**

where $\delta_h$ is a positive number to ensure the feasibility of the equation as constraint violation equal to zero. Assume that $\forall \overline{X_i} \in \mathrm{PS}, \mathrm{CV}_h(\overline{X_i}) \neq 0$, $\delta_h$ is defined as follows:

$$\delta_h = \begin{cases} 1, & \sum_{i=1}^{\mathrm{PS}} \mathrm{CV}_h(X_i) = 0; \\ 0.1 \min\limits_i \mathrm{CV}_h(\overline{X_i}), & \text{other} \end{cases} \tag{28}$$

In Eq. (27), $\varepsilon_j$ is a factor to adjust the selection probability adaptively. In general, an individual that maintains the dominance continuously may be a local optima. To avoid consuming more computation cost on it, its selection probability shall be reduced to a certain extent. Denote $C_j$ as the times that $X_j$ is not replaced by its offspring and $C^{\max}$ as a preset threshold. If $C_j > C^{\max}$, $X_j$ is regarded as a local optimum and impossible to be selected as a parent in neighborhood search operator, thus, $\varepsilon_j = 0$. As $C_j \in [0, C^{\max})$, the selection probability of $X_j$ becomes smaller with the increase of $C_j$. Based on this, $\varepsilon_j$ is calculated as follows:

$$\varepsilon_j = \begin{cases} 1 - \left(\frac{C_j}{C^{\max}}\right)^{(C^{\max} - C_j)}, & C_j \leqslant C^{\max}; \\ 0, & \text{other} \end{cases} \tag{29}$$

Then, an individual is selected by roulette wheel for exploitation in terms of its probability after normalization. The pseudocode of onlooker phase with adaptive selection probability is listed in Algorithm 3.

**Algorithm 3 Onlooker phase with adaptive selection probability (OP-ASP)**

**Input:** $X, C_i, C^{\max}$

**Output:** $X, C_i$

**For** $i = 1$ to PS
  Select $X_j$ by roulette wheel in terms of $P_j$;
  Produce $X_j^{\mathrm{new}}$ by neighborhood search on $X_j$;
  Evaluate $F(X_j^{\mathrm{new}})$ and $\mathrm{CV}_h(X_j^{\mathrm{new}})$;
  Update $X_j$ by Eq. (26);
  **If** $X_j \leftarrow X_j^{\mathrm{new}}$
    $C_j \leftarrow 0$;
  **Else**
    $C_j \leftarrow C_j + 1$;
**End for**

### 4.4 Knowledge-driven scout phase

Escaping from the local optimum is the main task for a scout. Generally, a new individual is generated randomly to replace the stagnant one, which contributes to a good diversity for the population. However, the new one may be infeasible for an optimization problem with constraint, thus providing the useless information for the evolution and slowing down the convergence.

To address the issue, a knowledge-driven initialization strategy is put forward to produce a new individual instead of the local optimum. Assuming that the segment corresponding to the service order of the $k$-th ETRV is $X_{ik} = \{\mathrm{sn}_{j_1+j_2+\cdots+j_{k-1}+1}, \mathrm{sn}_{j_1+j_2+\cdots+j_{k-1}+2}, \ldots, \mathrm{sn}_{j_1+j_2+\cdots+j_k}\}$ and there are $K$ segments in a solution. Knowledge refers to a segment that appears at the higher frequency among individuals, represented by $\{\mathrm{sn}_l, \mathrm{sn}_{l+1}, \ldots, \mathrm{sn}_{l+m}\}$. Its implicit information may provide valuable guidance for producing a feasible and superior individual[72]. During the evolution, all segments in feasible $X_i$ satisfying $\forall h$, $\mathrm{CV}_h(X_i)=0$ are extracted from the current population, and the high-frequency ones are retained as knowledge by frequent pattern mining. The segment that has the highest frequency is then selected as the most valuable knowledge to form a new individual. In order to guarantee the diversity, the rest service nodes are randomly assigned. If the new one dissatisfies any constraint, the repair operator[73] is carried on to split the permutation of other nodes into a set of routes based on constraints and obtain a feasible one finally. The psseudocode of knowledge-driven scout phase is listed in Algorithm 4.

## 5 Simulation Results and Discussion

To verify the rationality of improved artificial bee

**Algorithm 4 Knowledge-driven scout phase (KSP)**

**Input:** $X$, $C$, $C^{\max}$

**Output:** $X$, $C$

**For** $i$ = 1 to PS

  **If** $C_i \geqslant C^{\max}$

    Extract all segments of feasible individuals $\forall X_j \in X$, $\sum_h \mathrm{CV}_h(X_j) = 0$;

    Select the high-frequency segment $\{\mathrm{sn}_l, \mathrm{sn}_{l+1}, \ldots, \mathrm{sn}_{l+m}\}$ by frequent pattern mining;

    Arrange the remaining nodes in random order $\{\mathrm{sn}_1, \mathrm{sn}_2, \ldots, \mathrm{sn}_N\} \backslash \{\mathrm{sn}_l, \mathrm{sn}_{l+1}, \ldots, \mathrm{sn}_{l+m}\}$;

    Split the permutation of the remaining nodes based on three constraints;

    Obtain a feasible solution to replace $X_i$

  **End if**

**End for**

colony algorithm proposed in the paper, three groups of experiments are done on a real-world LRPETRV derived from a coal mine in Shanxi Province. All experiments are conducted on MATLAB R2018a with Intel(R) Core(TM) i7-10750H CPU @2.60 GHz, 16.00 GB RAM. Each algorithm has been run 10 times independently, and Wilcoxon rank-sum test at 5% significance level is introduced to analyze the significant difference among the algorithm performance.

### 5.1 Instance description and parameter setting

Figure 1 depicts the layout of all roadways in a real-world LRPETRV. There are 36 sections of roadway in the coal mine, and they are connected with each other by linking nodes. Each roadway has its special gradient, maximum allowable speed, rolling resistance coefficient, and length, as listed in Table 1. A service task may be located in a roadway or completed in a linking node. Some instant using material will be transported to the corresponding operation point located in roadway, while some reusable material will be stored in storage place in a linking node. Each service task is denoted as a service node labelled by "star" shown in Fig. 1, and its information on demand and service time are listed in Table 2. According to the number of service nodes online, four instances with 15, 20, 25, and 30 service nodes, respectively, are formed for experimental analysis.

In all instances, 15 ETRVs with the same characteristics are employed to complete the service tasks. The main parameters of an ETRV are listed as follows: mass is 9100 kg, maximum load $Q$=5000 kg, battery capacity $B$=128 000 W·h, frontal area $F_{\mathrm{A}}$= 3.37 m$^2$, resistance coefficient of air $C_d$=0.78, auxiliary power $p_{\mathrm{A}}$=5 kW, mechanical transmission efficiency $\eta_1$=0.95, motor efficiency $\eta_2$=0.95, and energy recovery efficiency $\eta_3$=0.05.

During the experiments, four commonly-used population-based intelligent optimization algorithms, including genetic algorithm (GA)[74], particle swarm optimization (PSO)[75], ant colony optimization

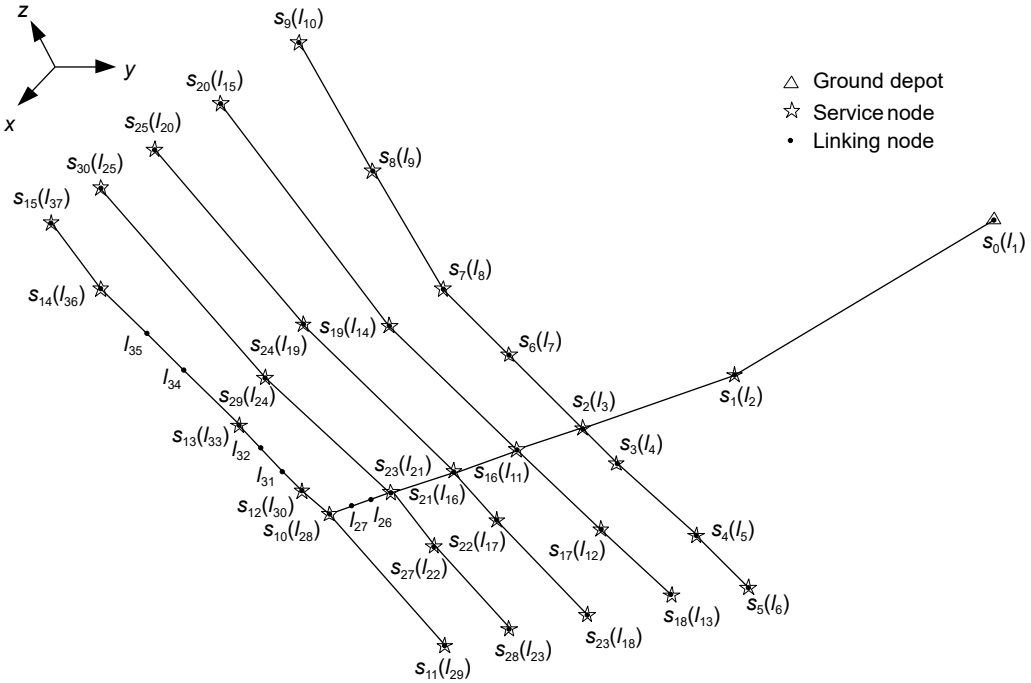


**Fig. 1 Layout of roadways in a real-world LRPETRV.**

**Table 1 Characteristics of roadways.**

| Roadway No. | Gradient (°) | Maximum allowable speed (km/h) | Rolling resistance coefficient | Length (m) |
|---|---|---|---|---|
| $r_{1,2}$ | −14 | 15 | 0.015 | 3348 |
| $r_{2,3}$ | 0 | 25 | 0.015 | 1800 |
| $r_{3,4}$ | 9 | 10 | 0.15 | 400 |
| $r_{4,5}$ | 7 | 10 | 0.015 | 1600 |
| $r_{5,6}$ | 7 | 10 | 0.015 | 600 |
| $r_{3,7}$ | −7 | 15 | 0.015 | 1200 |
| $r_{7,8}$ | −7 | 15 | 0.015 | 1000 |
| $r_{8,9}$ | 7 | 15 | 0.015 | 1600 |
| $r_{9,10}$ | 7 | 15 | 0.015 | 1600 |
| $r_{3,11}$ | 0 | 25 | 0.015 | 750 |
| $r_{11,12}$ | 9 | 10 | 0.015 | 1400 |
| $r_{12,13}$ | 7 | 10 | 0.015 | 1000 |
| $r_{11,14}$ | −7 | 15 | 0.015 | 2000 |
| $r_{14,15}$ | 7 | 15 | 0.015 | 3200 |
| $r_{11,16}$ | 0 | 25 | 0.015 | 750 |
| $r_{16,17}$ | 7 | 10 | 0.015 | 600 |
| $r_{17,18}$ | 7 | 10 | 0.015 | 1600 |
| $r_{16,19}$ | −7 | 15 | 0.015 | 2600 |
| $r_{19,20}$ | 7 | 15 | 0.015 | 2400 |
| $r_{16,21}$ | 0 | 25 | 0.015 | 750 |
| $r_{21,22}$ | 7 | 10 | 0.015 | 800 |
| $r_{22,23}$ | 7 | 10 | 0.015 | 1200 |
| $r_{21,24}$ | −7 | 15 | 0.015 | 2000 |
| $r_{24,25}$ | 7 | 15 | 0.015 | 2800 |
| $r_{21,26}$ | 0 | 25 | 0.015 | 400 |
| $r_{26,27}$ | −5 | 15 | 0.015 | 200 |
| $r_{27,28}$ | −7 | 15 | 0.015 | 150 |
| $r_{28,29}$ | 7 | 10 | 0.15 | 2000 |
| $r_{28,30}$ | −7 | 15 | 0.022 | 300 |
| $r_{30,31}$ | −7 | 15 | 0.022 | 500 |
| $r_{31,32}$ | 0 | 25 | 0.022 | 300 |
| $r_{32,33}$ | −5 | 15 | 0.022 | 200 |
| $r_{33,34}$ | −7 | 15 | 0.022 | 1000 |
| $r_{34,35}$ | −2 | 15 | 0.022 | 1200 |
| $r_{35,36}$ | 7 | 15 | 0.022 | 300 |
| $r_{36,37}$ | 1 | 15 | 0.011 | 800 |

(ACO)[76], and artificial bee colony (ABC)[77], are selected as the compared problem-solvers. To ensure the fairness of comparison, the main parameters of all comparative algorithms are set as suggested in their source except for population size and the maximum termination iteration. The main parameters of the proposed IABC are set as follows: population size PS=50, the maximum termination iteration Maxgen=30, the threshold $C^{\max}$=8, and the weight $w$=0.4.

**Table 2 Information of service nodes.**

| Node No. | $Q_{mi}$ (kg) | ST (s) | Node No. | $Q_{mi}$ (kg) | ST (s) |
|---|---|---|---|---|---|
| $s_1$ | 100 | 90 | $s_{16}$ | 1000 | 90 |
| $s_2$ | 1100 | 90 | $s_{17}$ | 900 | 90 |
| $s_3$ | 700 | 90 | $s_{18}$ | 1500 | 90 |
| $s_4$ | 800 | 90 | $s_{19}$ | 700 | 90 |
| $s_5$ | 1400 | 90 | $s_{20}$ | 2000 | 90 |
| $s_6$ | 2100 | 90 | $s_{21}$ | 1000 | 90 |
| $s_7$ | 400 | 90 | $s_{22}$ | 800 | 90 |
| $s_8$ | 800 | 90 | $s_{23}$ | 1500 | 90 |
| $s_9$ | 100 | 90 | $s_{24}$ | 1000 | 90 |
| $s_{10}$ | 500 | 90 | $s_{25}$ | 2000 | 90 |
| $s_{11}$ | 600 | 90 | $s_{26}$ | 1000 | 90 |
| $s_{12}$ | 1200 | 90 | $s_{27}$ | 800 | 90 |
| $s_{13}$ | 1300 | 90 | $s_{28}$ | 1500 | 90 |
| $s_{14}$ | 1300 | 90 | $s_{29}$ | 1500 | 90 |
| $s_{15}$ | 2500 | 90 | $s_{30}$ | 2000 | 90 |

### 5.2 Sensitivity analysis of main parameters in IABC

In IABC, the threshold $C^{\max}$ determines the maximum number of neighborhood search on a food source. An individual will be abandoned if its quality has not been improved by consecutive $C^{\max}$ neighborhood search, which plays a direct impact on the diversity of population and convergence.

As $C^{\max}$ varies from 4 to 12 every 1, the mean of objective values for the best solutions obtained by IABC is normalized. Figure 2 depicts mean of energy consumption after normalization under various $C^{\max}$ on four instances. We observe from the curve that the algorithm performance is sensitive to $C^{\max}$, and energy consumption is the least as $C^{\max}$ = 8 for most instances. Under too smaller $C^{\max}$, the exploitation on the current food source is insufficient, slowing down the convergence speed. With the increase of $C^{\max}$, local search for a food source becomes better, however, the exploration may be weak, causing the risk of premature convergence.

$w$ represents the weight of the historical contribution for each neighborhood search operator in the employed bee phase. As $w$ varies from 0.1 to 0.9 every 0.1, the mean of energy consumption after normalization for the optima obtained by IABC is shown in Fig. 3. Apparently, the best algorithm performance is achieved as $w$ = 0.4, except for Instance 15. Under too smaller $w$,

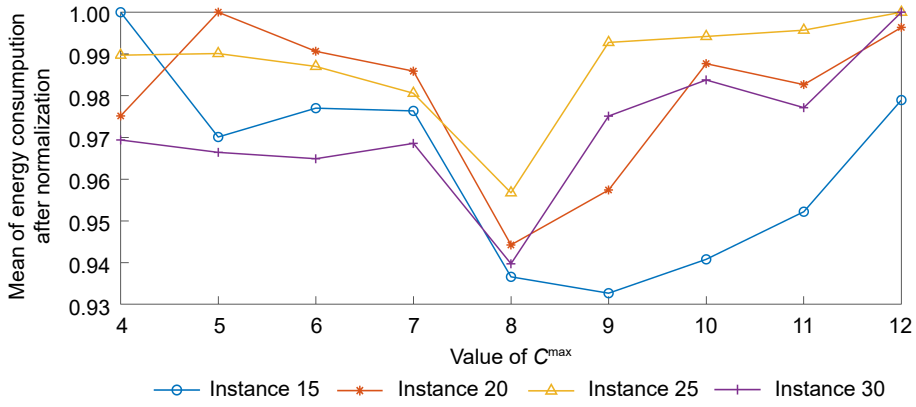


**Fig. 2 Mean of energy consumption after normalization obtained by IABC under different $C^{max}$ on four instances.**

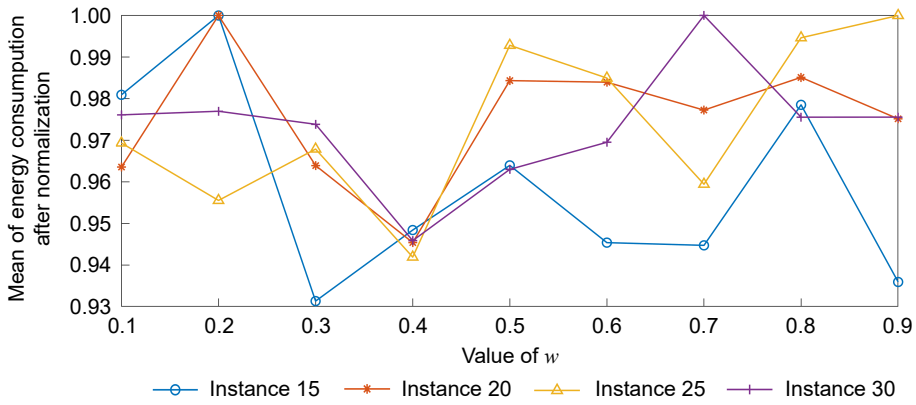


**Fig. 3 Mean of energy consumption after normalization obtained by IABC under different $w$ on four instances.**

the historical performance of operators plays a tiny role in their selection. On the contrary, the usability of operators on the current search space becomes less on larger $w$. During the evolution, the most appropriated operation is selected by trading off its historical contribution and current score.

### 5.3 Effectiveness of newly-designed strategies

In three phases of IABC, we designed three specific strategies, including adaptive neighborhood search for employed bees, adaptive selection probability for onlookers, and knowledge-driven initialization for scouts. In order to verify their effectiveness, three variants of IABC are introduced. IABC/ANS removes adaptive neighborhood search and adopts swapping operator in employed bee phase. IABC/ASP sets the adaptive factor of adaptive selection probability for onlookers to 1. IABC/KDI employs random generation method instead of a knowledge-driven initialization strategy in scout phase.

The mean of the optima obtained by IABC and its variants on each instance and their significance test are shown in Table 3, where "+" indicates that IABC is significantly superior to other variants in terms of Wilcoxon rank-sum test. Intuitively, IABC achieves the most competitive solutions on all instances and is significantly better than its variants. This proves that three newly-designed strategies are helpful to effectively enhance the algorithm performance.

To further analyze the rationality of three strategies

**Table 3 Comparison of energy consumption obtained by IABC and its variants.**

| Problem | $F$ (kW·h) | | | |
|---|---|---|---|---|
| | IABC/ANS | IABC/ASP | IABC/KDI | IABC |
| Instance 15 | 248.40+ | 256.87+ | 252.11+ | **242.35** |
| Instance 20 | 388.76+ | 407.98+ | 393.18+ | **379.47** |
| Instance 25 | 522.95+ | 546.01+ | 539.93+ | **505.08** |
| Instance 30 | 663.19+ | 695.11+ | 698.94+ | **653.56** |

proposed in the paper, the number of adopting each neighborhood search operator during the evolution on all instances is shown in Fig. 4. Apparently, the most suitable operator for neighbor search is adaptively adjusted in terms of its comprehensive performance.

Figure 5 depicts the number of effective neighborhood searches (ENSs) in onlooker phase during the evolution of IABC and IABC/ASP, as well as the number of feasible solutions (FSs) obtained by IABC and IABC/KDI in each iteration. The so-called effective neighborhood search in onlooker phase is that a new individual obtained by this operator has less energy consumption than its parent. Intuitively, the number of ENSs for both IABC and IABC/ASP becomes smaller during the evolution. In the early stage of evolution, IABC significantly performs more effective neighborhood searches than IABC/ASP on all instance and achieves the competitive search efficiency. Based on adaptive selection probability, IABC can adjust onlookers searching for a promising food source rather than a local optima. Being different from it, IABC/ASP determines the selection probability according to the quality of individuals and gives no consideration on the risk of trapping into local optimal. Thus, the number of ENSs for IABC/ASP decreases quickly, easily causing premature convergence.

As shown in Fig. 5, the number of feasible solutions increases quickly to the maximal size and remains stable during the evolution of IABC. On the contrary, IABC/KDI produces the smaller number of feasible solutions than IABC because a new individual is generated randomly, which slows down the convergence. More especially, this divergence becomes more significant with the increasing number of service

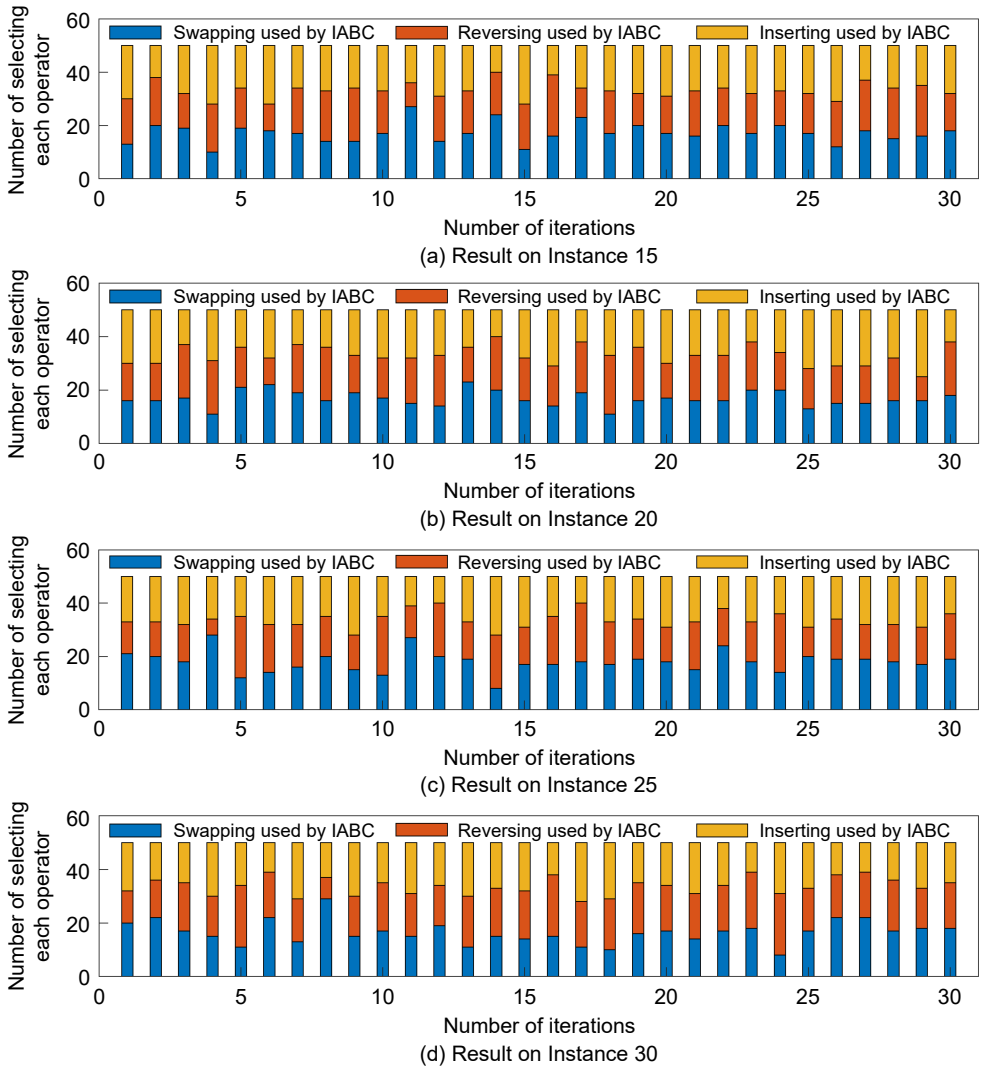


**Fig. 4 Number of selecting each neighborhood search operator during the evolution.**

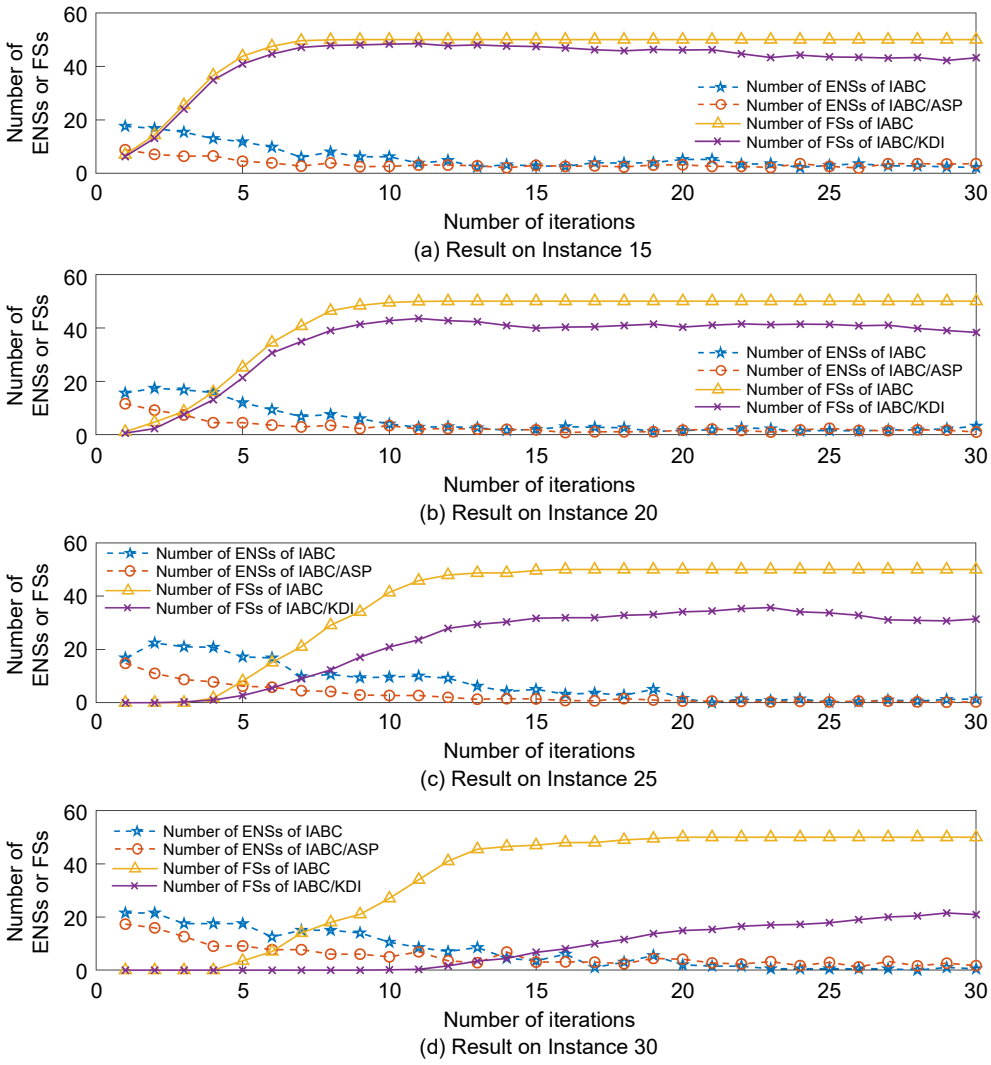


**Fig. 5 Number of ENSs in onlooker phase and FSs during the evolution.**

nodes. The knowledge-driven initialization strategy designed in IABC utilizes the valuable information and a repair operator to produce a feasible solution. This contributes to not only a good diversity of the population, but also higher evolutionary efficiency.

### 5.4 Performance comparison among various algorithms

In this subsection, IABC is compared with four popular swarm intelligent optimization algorithms. Table 4 shows statistical results obtained by different algorithms. In 10 times of experiments for each algorithm on each instance, the ratio of the number of experiments that achieve feasible solutions successfully is counted and denoted as SR. Wilcoxon rank-sum test is performed between the successful experiments of the compared algorithms and that of IABC, where "+" indicates that IABC is significantly superior to the comparative algorithms in terms of Wilcoxon rank-sum test.

**Table 4 Comparison of the optimal solutions among different algorithms.**

| Problem | GA | | PSO | | ACO | | ABC | | IABC | |
|---|---|---|---|---|---|---|---|---|---|---|
| | $F$ (kW·h) | SR (%) | $F$ (kW·h) | SR (%) | $F$ (kW·h) | SR (%) | $F$ (kW·h) | SR (%) | $F$ (kW·h) | SR (%) |
| Instance 15 | 316.18+ | 100 | 252.33+ | 100 | 314.22+ | 100 | 261.20+ | 100 | **242.35** | 100 |
| Instance 20 | 470.28+ | 100 | 399.38+ | 100 | 520.02+ | 100 | 398.96+ | 100 | **379.47** | 100 |
| Instance 25 | 621.52+ | 80 | 521.53+ | 90 | − | 0 | 540.45+ | 100 | **505.08** | 100 |
| Instance 30 | 703.67+ | 30 | 690.97+ | 100 | − | 0 | 683.86+ | 90 | **653.56** | 100 |

We observe from Table 4 that IABC can successfully obtain feasible solutions at each running and achieve the superior solution on each instance. Apparently, IABC provides the competitive performance due to three newly-designed strategies. No matter which kind of comparative algorithm, the success ratio of achieving feasible solutions all decreases with the increasing number of service nodes. Compared with GA and PSO, ACO shows the worst performance and only solves Instance 15 and Instance 20 due to its strong dependency on the initial pheromone table. In large-scale instances, the fixed number of ETRVs completes the variable service tasks, thus, randomly generating a feasible solution is difficult, forming an initial population with worse quality.

Furthermore, the best routes of ETRVs in 10 times of experiments for IABC on each instance are shown in Figs. 6–9. {0, 1, 6, 3, 12, 9, 8, 0, 7, 13, 5, 4, 2, 0, 15, 14, 10, 11, 0} is the optimal route obtained by IABC on Instance 15, in which three ETRVs are employed to serve 15 service nodes and the sub-routes for each ETRV are $0 \to 1 \to 6 \to 3 \to 12 \to 9 \to 8 \to 0$, $0 \to 7 \to 13 \to 5 \to 4 \to 2 \to 0$, and $0 \to 15 \to 14 \to 10 \to 11 \to 0$, as shown in Fig. 6. Likewise, the optimal routes obtained by IABC on other three instances are {0, 18, 17, 4, 2, 1, 0, 3, 20, 19, 9, 8, 0, 15, 16, 0, 5, 6, 7, 0, 10, 14, 13, 11, 12, 0}, {0, 3, 19, 20, 4, 0, 6, 1, 0, 7, 8, 9, 5, 0, 10, 23, 18, 0, 15, 14, 11, 0, 2, 21, 0, 17, 13, 12, 0, 22, 16, 25, 24, 0}, and {0, 28, 30, 9, 10, 0, 23, 26, 18, 0, 11, 29, 25, 4, 0, 27, 19, 17, 5, 3, 7, 0, 2, 15, 14, 0, 24, 8, 21, 1, 20, 0, 16, 22, 6, 0, 12, 13, 0}, respectively. Figures 7–9 depict their routes. We observe from Figs. 6–9 that the number of service tasks that are assigned to each ETRV is similar on Instance 15. With the increasing number of service nodes, the amount of tasks served by ETRVs are quite different from each other. Moreover, various ETRVs may share the same segment or sub-segment in their routes due to the limit of vehicle avoidance.

## 6 Conclusion

In an auxiliary transportation system of inclined-shaft coal mines, there are some scenario-specific regulation and limitation for scheduling ETRVs. Taking transportation safety and efficiency into account, we formulate a low-carbon ETRV routing to single-optimization problem with constraints. The optimization objective focuses on the total energy consumption that synchronously reflects the economic cost and carbon emission. More especially, energy

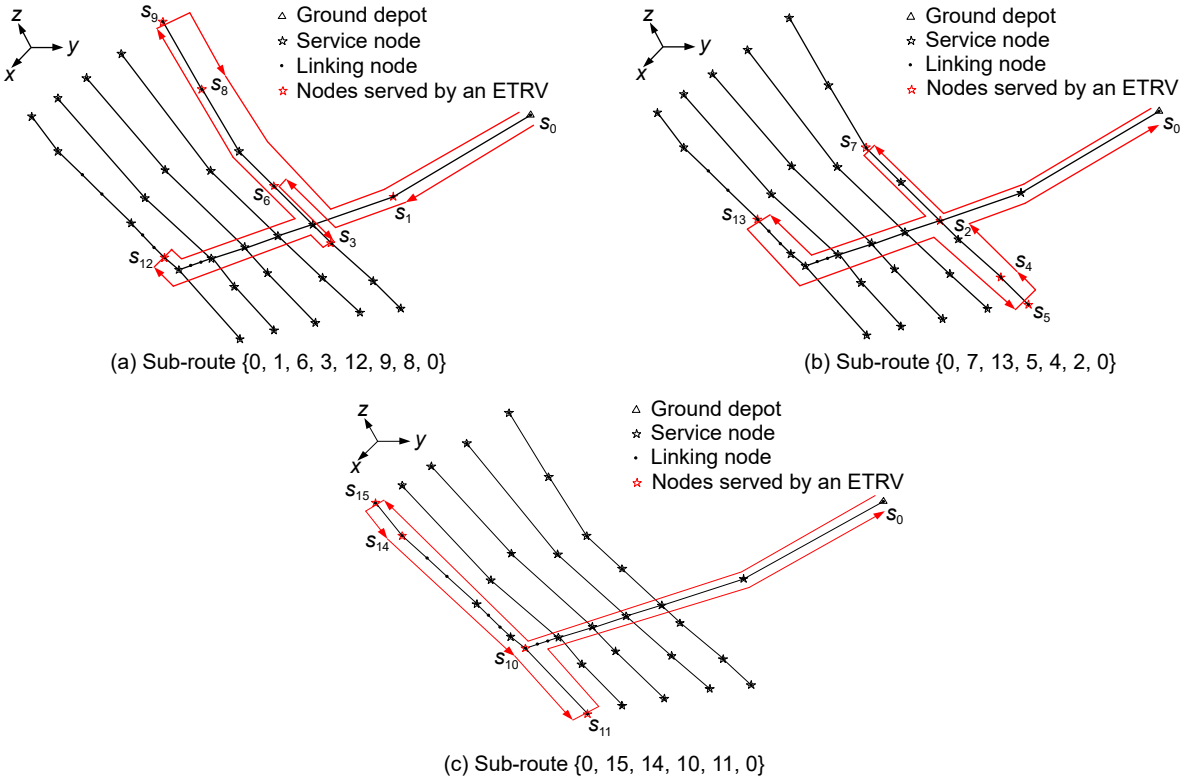


(a) Sub-route {0, 1, 6, 3, 12, 9, 8, 0}

(b) Sub-route {0, 7, 13, 5, 4, 2, 0}

(c) Sub-route {0, 15, 14, 10, 11, 0}

**Fig. 6 Optimal routes obtained by IABC on Instance 15.**

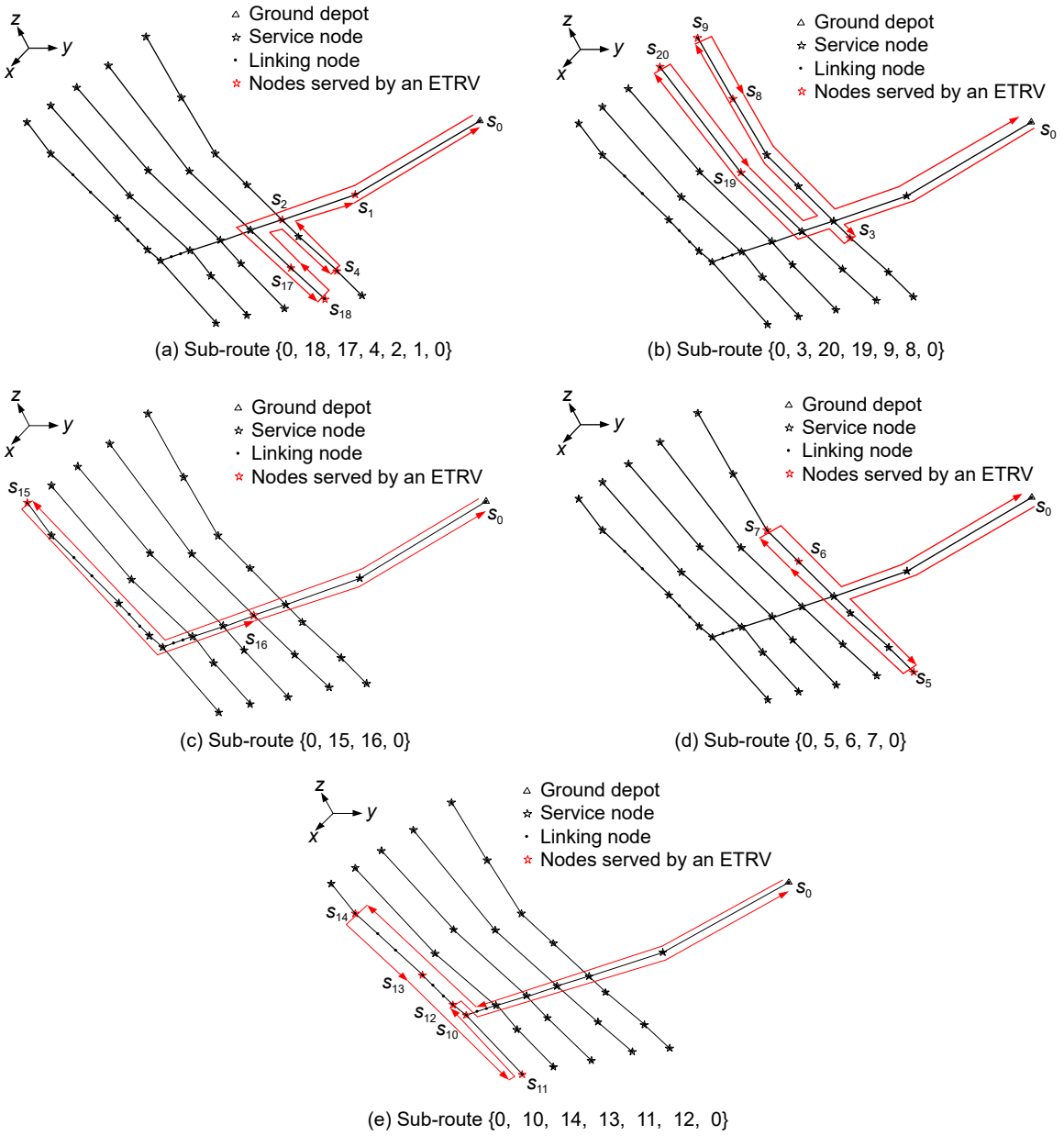


(a) Sub-route {0, 18, 17, 4, 2, 1, 0}

(b) Sub-route {0, 3, 20, 19, 9, 8, 0}

(c) Sub-route {0, 15, 16, 0}

(d) Sub-route {0, 5, 6, 7, 0}

(e) Sub-route {0, 10, 14, 13, 11, 12, 0}

**Fig. 7 Optimal routes obtained by IABC on Instance 20.**

consumption of an ETRV driving in a roadway is modeled in terms of its load, the driving mode, and road condition. Due to multiple constraints, seeking the optimal feasible route of ETRVs is a challenging problem. To address the issue, an improved ABC with three newly-designed strategies is put forward. The statistical experimental results on four practical instances show that IABC is superior to four comparative algorithms on convergence and success rate. More especially, both adaptive neighborhood search and adaptive selection probability are helpful to improve search efficiency. Knowledge-driven initialization produces more diverse and feasible individual for a population. Though IABC provides a promising problem-solver for routing ETRVs, scheduling heterogeneous TRVs that have various power is our future work.

## Acknowledgment

This work was supported by the National Key R&D Program of China (No. 2022YFB4703701), National Natural Science Foundation of China (Nos. 61973305, 52121003, and 61573361), Royal Society International Exchanges 2020 Cost Share, and the 111 Project (No. B21014).

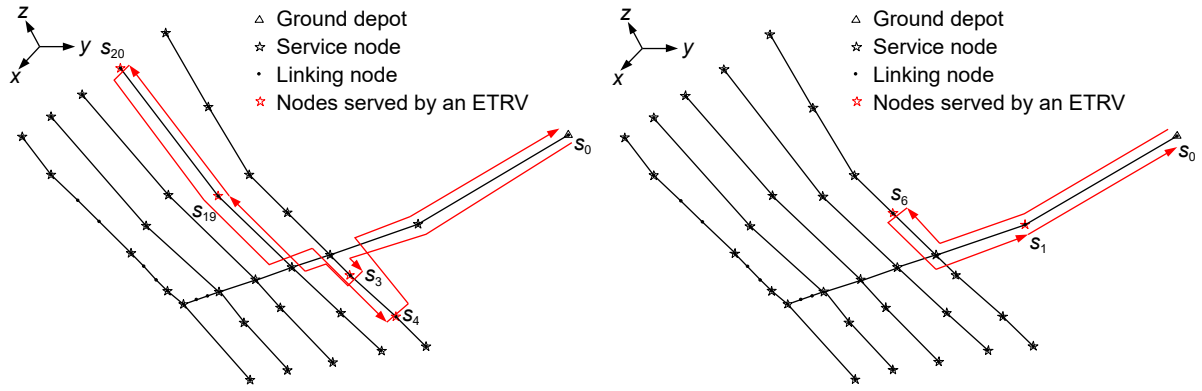


(a) Sub-route {0, 3, 19, 20, 4, 0}




(b) Sub-route {0, 6, 1, 0}

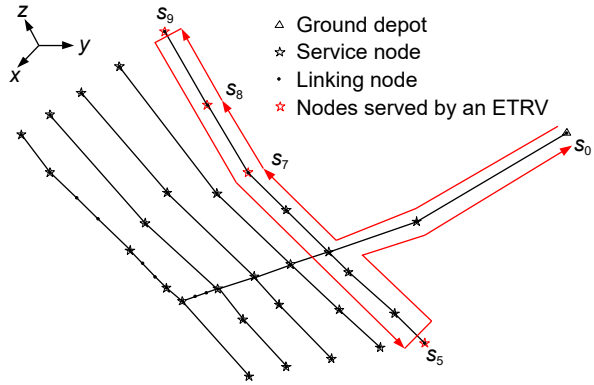


(c) Sub-route {0, 7, 8, 9, 5, 0}

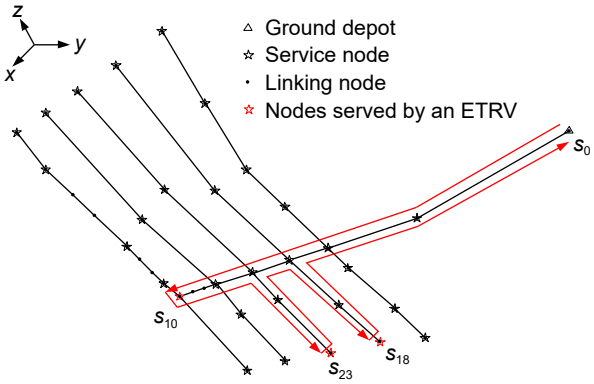


(d) Sub-route {0, 10, 23, 18, 0}

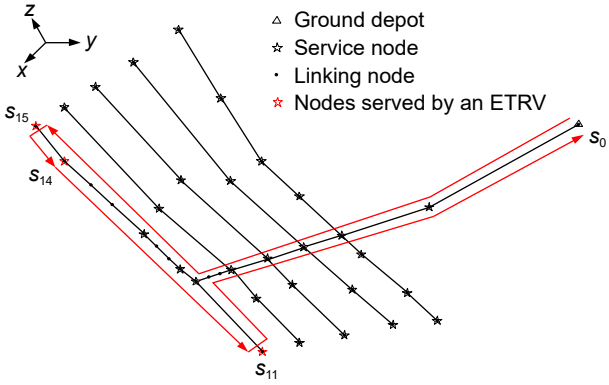


(e) Sub-route {0, 15, 14, 11, 0}

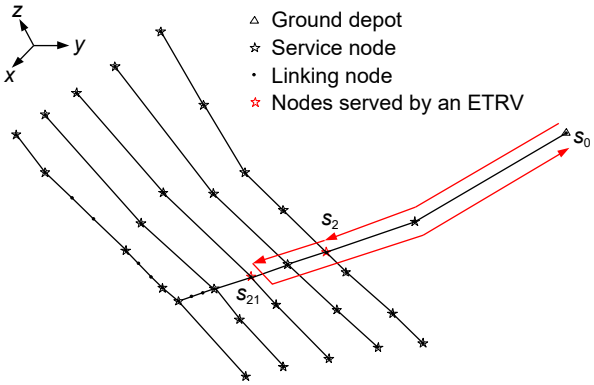


(f) Sub-route {0, 2, 21, 0}

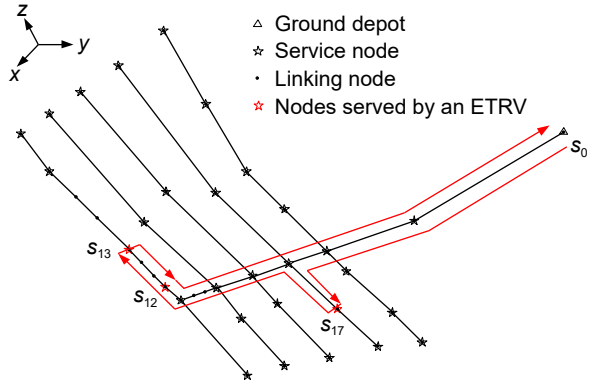


(g) Sub-route {0, 17, 13, 12, 0}

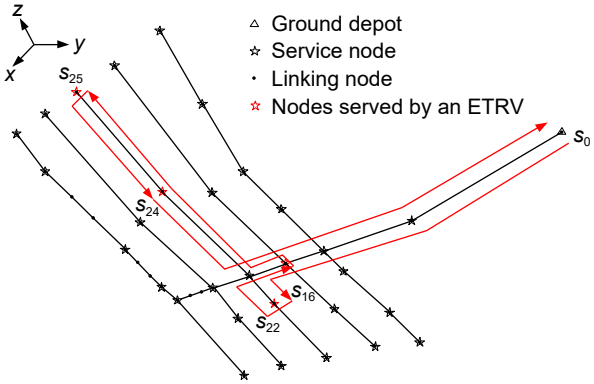


(h) Sub-route {0, 22, 16, 25, 24, 0}

**Fig. 8 Optimal routes obtained by IABC on Instance 25.**

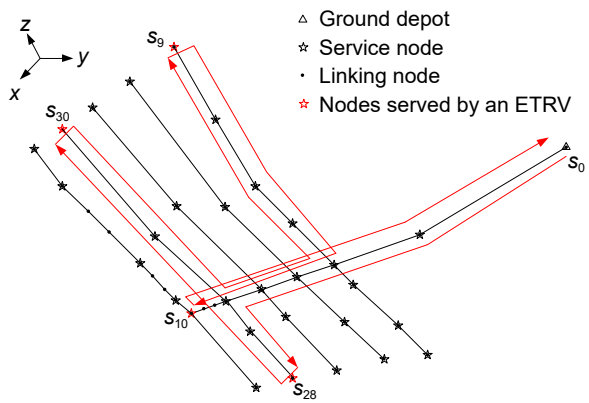


(a) Sub-route {0, 28, 30, 9, 10, 0}

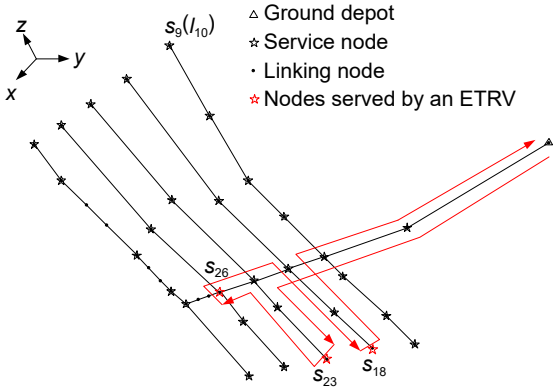


(b) Sub-route {0, 23, 26, 18, 0}

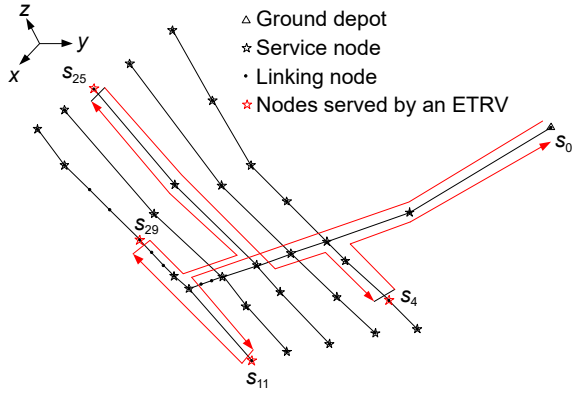


(c) Sub-route {0, 11, 29, 25, 4, 0}

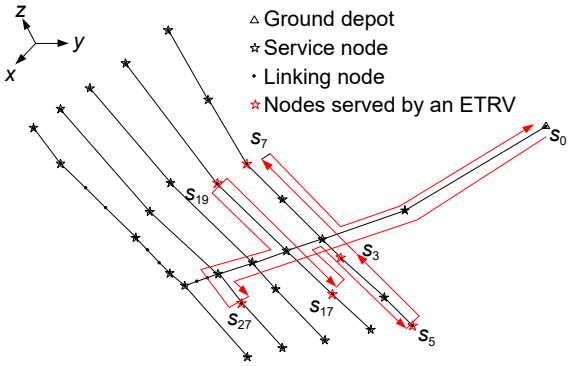


(d) Sub-route {0, 27, 19, 17, 5, 3, 7, 0}

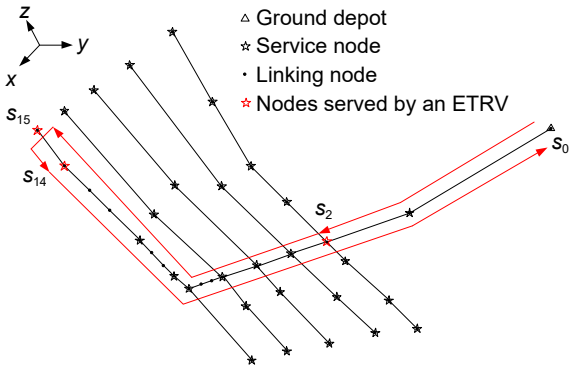


(e) Sub-route {0, 2, 15, 14, 0}

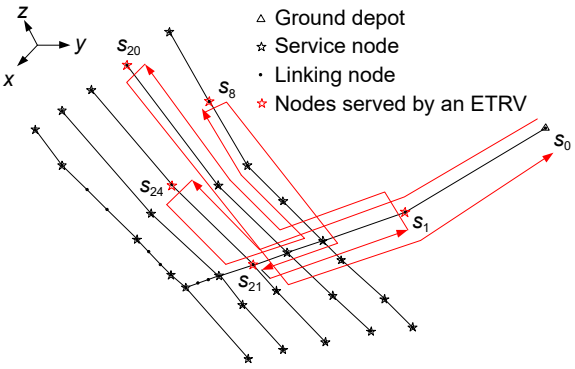


(f) Sub-route {0, 24, 8, 21, 1, 20, 0}

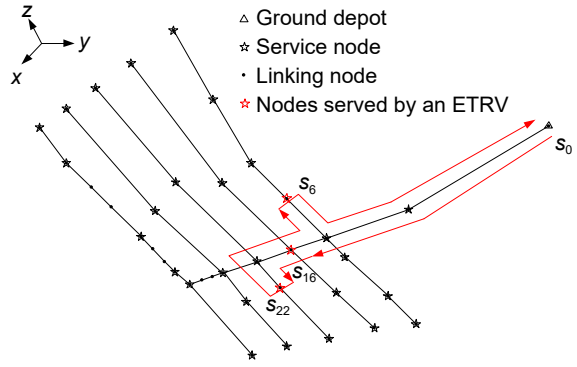


(g) Sub-route {0, 16, 22, 6, 0}

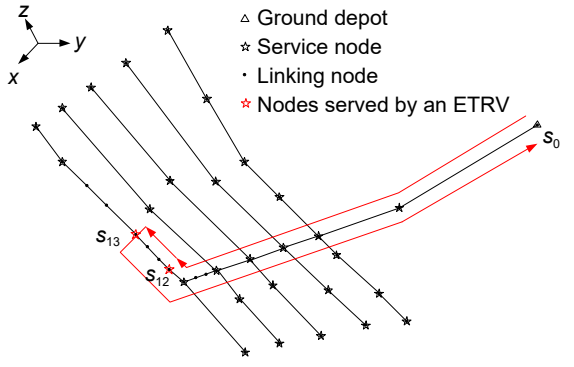


(h) Sub-route {0, 12, 13, 0}

**Fig. 9 Optimal routes obtained by IABC on Instance 30.**

## References


[1] F. Guo, F. Gao, S. Guo, and H. G. Ma, Research on the transport line of the trackless rubber tire vehicle underground coal mine, *Appl. Mech. Mater.*, vols. 373–375, pp. 2284–2287, 2013.

[2] J. Bao, S. Yang, S. Ge, P. Han, and Y. Yin, Dynamic performance of an underground trackless rubber tyred vehicle driven by flameproof diesel engine, *Teh. Vjesn.*, vol. 24, pp. 279–286, 2017.

[3] X. Yuan, Y. Lu, J. Bao, P. Han, Y. Yin, and X. Wang, Design and optimization on the degree of hybridization of underground hybrid electric trackless rubber-tyred vehicle, *Energies*, vol. 15, no. 18, p. 6544, 2022.

[4] B. Yan, B. Han, J. Wang, and D. Sun, Vibration isolation analysis of tubular sandwiched structure used for trackless rubber-tyred vehicles, *Polym. Polym. Compos.*, vol. 26, nos. 5&6, pp. 380–388, 2018.

[5] C. Liu, W. Nie, X. Liu, Y. Hua, W. Zhou, F. Yu, W. Niu, N. Sun, and Q. Xue, Behavior of the particulate matter (PM) emitted by trackless rubber-tyred vehicle (TRTV) at an idle speed under different movement conditions and ventilation optimization, *Sci. Total Environ.*, vol. 783, p. 147008, 2021.

[6] C. Du, Design of anti-collision device of mine trackless rubber tire vehicle, *IOP Conf. Ser.*: *Earth Environ. Sci.*, vol. 508, p. 012212, 2020.

[7] P. Han, J. Bao, S. Ge, Y. Yin, C. Ma, and S. Yang, Parameter design of an ISG hybrid electric trackless rubber tyred vehicle based on degree of hybridisation, *Int. J. Heavy Veh. Syst.*, vol. 24, no. 3, pp. 239–259, 2017.

[8] Y. Zhou, W. Zhou, X. Lu, I. M. Jiskani, Q. Cai, P. Liu, and L. Li, Evaluation index system of green surface mining in China, *Min. Metall. Explor.*, vol. 37, no. 4, pp. 1093–1103, 2020.

[9] L. Dong, D. Sun, W. Shu, and X. Li, Exploration: Safe and clean mining on Earth and asteroids, *J. Clean. Prod.*, vol. 257, p. 120899, 2020.

[10] Z. Cai, Research on dispatching system of trackless rubber wheel car in underground coal mine, (in Chinese), MSc dissertation, School of Mechanical Engineering, Xi'an University of Science & Technology, Xi'an, China, 2019.

[11] C. Han, Research on intelligent dispatching management system of mine trackless rubber wheeler, (in Chinese), *Mechanical and Electrical Engineering Technology*, vol. 49, no. 9, pp. 131–133, 2020.

[12] B. Zhou, L. Tang, and S. Liu, Design of path planning underground vehicle based on genetic algorithm, (in Chinese), *Coal Mine Machinery*, vol. 43, no. 1, pp. 23–26, 2022.

[13] Y. Zhou, J. Huang, J. Shi, R. Wang, and K. Huang, The electric vehicle routing problem with partial recharge and vehicle recycling, *Complex Intell. Syst.*, vol. 7, no. 3, pp. 1445–1458, 2021.

[14] M. Keskin, G. Laporte, and B. Çatay, Electric vehicle routing problem with time-dependent waiting times at recharging stations, *Comput. Oper. Res.*, vol. 107, pp. 77–94, 2019.

[15] C. Yao, S. Chen, and Z. Yang, Joint routing and charging problem of multiple electric vehicles: A fast optimization algorithm, *IEEE Trans. Intell. Transp. Syst.*, vol. 23, no. 7, pp. 8184–8193, 2022.

[16] C. Lee, An exact algorithm for the electric-vehicle routing problem with nonlinear charging time, *J. Oper. Res. Soc.*, vol. 72, no. 7, pp. 1461–1485, 2021.

[17] M. A. Akbay, C. B. Kalayci, C. Blum, and O. Polat, Variable neighborhood search for the two-echelon electric vehicle routing problem with time windows, *Appl. Sci.*, vol. 12, no. 3, p. 1014, 2022.

[18] Y. Zhu, C. Li, and K. Y. Lee, The NR-EGA for the EVRP problem with the electric energy consumption model, *Energies*, vol. 15, no. 10, p. 3681, 2022.

[19] Y. -H. Jia, Y. Mei, and M. Zhang, A bilevel ant colony optimization algorithm for capacitated electric vehicle routing problem, *IEEE Trans. Cybern.*, vol. 52, no. 10, pp. 10855–10868, 2022.

[20] A. Kumar, R. Kumar, and A. Aggarwal, A meta-heuristic-based energy efficient route modeling for EV on non-identical road surfaces, *Neural Comput. Appl.*, vol. 34, no. 18, pp. 15575–15588, 2022.

[21] X. Dong, Q. Lin, M. Xu, and Y. Cai, Artificial bee colony algorithm with generating neighbourhood solution for large scale coloured traveling salesman problem, *IET Intell. Transp. Syst.*, vol. 13, no. 10, pp. 1483–1491, 2019.

[22] Z. Nagy, Á. Werner-Stark, and T. Dulai, An artificial bee colony algorithm for static and dynamic capacitated arc routing problems, *Mathematics*, vol. 10, no. 13, p. 2205, 2022.

[23] Z. Gu, Y. Zhu, Y. Wang, X. Du, M. Guizani, and Z. Tian, Applying artificial bee colony algorithm to the multidepot vehicle routing problem, *Softw.*: *Practice and Experirence*, vol. 52, no. 3, pp. 756–771, 2022.

[24] Y. Li, Y. Shen, and J. Li, A discrete artificial bee colony algorithm for stochastic vehicle scheduling, *Complex System Modeling and Simulation*, vol. 2, no. 3, pp. 238–252, 2022.

[25] J. -J. Ji, Y. -N. Guo, X. -Z. Gao, D. -W. Gong, and Y. -P. Wang, Q-learning-based hyperheuristic evolutionary algorithm for dynamic task allocation of crowdsensing, *IEEE Trans*. *Cybern*., doi: 10.1109/TCYB.2021.3112675.

[26] R. Zhang, Research on operation performance detection and dispatching systems of trackless rubber-tyred vehicle, (in Chinese), MSc dissertation, School of Mechanical and Vehicle Engineering, Taiyuan University of Technology, Taiyuan, China, 2020.

[27] Y. -N. Guo, J. Cheng, S. Luo, D. Gong, and Y. Xue, Robust dynamic multi-objective vehicle routing optimization method, *IEEE/ACM Trans. Comput. Biol. Bioinform.*, vol. 15, no. 6, pp. 1891–1903, 2018.

[28] G. Ferro, M. Paolucci, and M. Robba, Optimal charging and routing of electric vehicles with power constraints and time-of-use energy prices, *IEEE Trans. Veh. Technol.*, vol. 69, no. 12, pp. 14436–14447, 2020.

[29] S. Karakatič, Optimizing nonlinear charging times of electric vehicle routing with genetic algorithm, *Expert Syst. Appl.*, vol. 164, p. 114039, 2021.

[30] Z. Yi and P. H. Bauer, Optimal stochastic eco-routing solutions for electric vehicles, *IEEE Trans. Intell. Transp. Syst.*, vol. 19, no. 12, pp. 3807–3817, 2018.

[31] X. Zhu, R. Yan, Z. Huang, W. Wei, J. Yang, and S.

Kudratova, Logistic optimization for multi depots loading capacitated electric vehicle routing problem from low carbon perspective, *IEEE Access*, vol. 8, pp. 31934–31947, 2020.

[32] G. Macrina, L. D. P. Pugliese, F. Guerriero, and G. Laporte, The green mixed fleet vehicle routing problem with partial battery recharging and time windows, *Comput. Oper. Res.*, vol. 101, pp. 183–199, 2019.

[33] T. Erdelić and T. Carić, Goods delivery with electric vehicles: Electric vehicle routing optimization with time windows and partial or full recharge, *Energies*, vol. 15, no. 1, p. 285, 2022.

[34] T. Erdelić and T. Carić, A survey on the electric vehicle routing problem: Variants and solution approaches, *J. Adv. Transp.*, vol. 2019, p. 5075671, 2019.

[35] H. R. Sayarshad, V. Mahmoodian, and H. O. Gao, Non-myopic dynamic routing of electric taxis with battery swapping stations, *Sustain. Cities Soc.*, vol. 57, p. 102113, 2020.

[36] D. G. Sánchez, A. Tabares, L. T. Faria, J. C. Rivera, and J. F. Franco, A clustering approach for the optimal siting of recharging stations in the electric vehicle routing problem with time windows, *Energies*, vol. 15, no. 7, p. 2372, 2022.

[37] J. Hof, M. Schneider, and D. Goeke, Solving the battery swap station location-routing problem with capacitated electric vehicles using an AVNS algorithm for vehicle-routing problems with intermediate stops, *Transp. Res. B*, vol. 97, pp. 102–112, 2017.

[38] S. Zhang, M. Chen, and W. Zhang, A novel location-routing problem in electric vehicle transportation with stochastic demands, *J. Clean. Prod.*, vol. 221, pp. 567–581, 2019.

[39] I. Kucukoglu, R. Dewil, and D. Cattrysse, The electric vehicle routing problem and its variations: A literature review, *Comput. Ind. Eng.*, vol. 161, p. 107650, 2021.

[40] A. Almouhanna, C. L. Quintero-Araujo, J. Panadero, A. A. Juan, B. Khosravi, and D. Ouelhadj, The location routing problem using electric vehicles with constrained distance, *Comput. Oper. Res.*, vol. 115, p. 104864, 2020.

[41] S. R. Kancharla and G. Ramadurai, Electric vehicle routing problem with non-linear charging and load-dependent discharging, *Expert Syst. Appl.*, vol. 160, p. 113714, 2020.

[42] R. Basso, B. Kulcsár, B. Egardt, P. Lindroth, and I. Sanchez-Diaz, Energy consumption estimation integrated into the electric vehicle routing problem, *Transp. Res. D*, vol. 69, pp. 141–167, 2019.

[43] T. Perger and H. Auer, Energy efficient route planning for electric vehicles with special consideration of the topography and battery lifetime, *Energy Effic.*, vol. 13, no. 8, pp. 1705–1726, 2020.

[44] S. Pelletier, O. Jabali, and G. Laporte, The electric vehicle routing problem with energy consumption uncertainty, *Transp. Res. B*, vol. 126, pp. 225–255, 2019.

[45] R. Basso, B. Kulcsár, and I. Sanchez-Diaz, Electric vehicle routing problem with machine learning for energy prediction, *Transp. Res. B*, vol. 145, pp. 24–55, 2021.

[46] J. Zhang, Z. Wang, P. Liu, and Z. Zhang, Energy consumption analysis and prediction of electric vehicles based on real-world driving data, *Appl. Energy*, vol. 275, p. 115408, 2020.

[47] M. R. C. O. Leite, H. S. Bernardino, and L. B. Gonçalves, A variable neighborhood descent with ant colony optimization to solve a bilevel problem with station location and vehicle routing, *Appl. Intell.*, vol. 52, no. 7, pp. 7070–7090, 2022.

[48] R. Zhang, J. Guo, and J. Wang, A time-dependent electric vehicle routing problem with congestion tolls, *IEEE Trans. Eng. Manag.*, vol. 69, no. 4, pp. 861–873, 2020.

[49] Y. Shen, L. Yu, and J. Li, Robust electric vehicle routing problem with time windows under demand uncertainty and weight-related energy consumption, *Complex System Modeling Simulation*, vol. 2, no. 1, pp. 18–34, 2022.

[50] M. Granada-Echeverri, L. C. Cubides, and J. O. Bustamante, The electric vehicle routing problem with backhauls, *Int. J. Ind. Eng. Comp.*, vol. 11, pp. 131–152, 2020.

[51] Y. Zhu, K. Y. Lee, and Y. Wang, Adaptive elitist genetic algorithm with improved neighbor routing initialization for electric vehicle routing problems, *IEEE Access*, vol. 9, pp. 16661–16671, 2021.

[52] S. Zhang, Y. Gajpal, S. S. Appadoo, and M. M. S. Abdulkader, Electric vehicle routing problem with recharging stations for minimizing energy consumption, *Int. J. Prod. Econ.*, vol. 203, pp. 404–413, 2018.

[53] B. -H. Zhou and F. Tan, Electric vehicle handling routing and battery swap station location optimisation for automotive assembly lines, *Int. J. Comput. Integr. Manuf.*, vol. 31, no. 10, pp. 978–991, 2018.

[54] D. Karaboga, An idea based on honey bee swarm for numerical optimization, Tech. Rep. TR06, Erciyes University, Kaiseri, Turkey, 2005.

[55] J. Cao, B. Yin, X. Lu, Y. Kang, and X. Chen, A modified artificial bee colony approach for the 0-1 knapsack problem, *Appl. Intell.*, vol. 48, no. 6, pp. 1582–1595, 2018.

[56] S. Zhang and S. Liu, A discrete improved artificial bee colony algorithm for 0–1 knapsack problem, *IEEE Access*, vol. 7, pp. 104982–104991, 2019.

[57] Y. He, H. Xie, T. -L. Wong, and X. Wang, A novel binary artificial bee colony algorithm for the set-union knapsack problem, *Future Gener. Comput. Syst.*, vol. 78, pp. 77–86, 2018.

[58] X. Chen, B. Xu, C. Mei, Y. Ding, and K. Li, Teaching-learning-based artificial bee colony for solar photovoltaic parameter estimation, *Appl. Energy*, vol. 212, pp. 1578–1588, 2018.

[59] X. Chen, X. Wei, G. Yang, and W. Du, Fireworks explosion based artificial bee colony for numerical optimization, *Knowl. Based Syst.*, vol. 188, p. 105002, 2020.

[60] F. Xu, H. Li, C. -M. Pun, H. Hu, Y. Li, Y. Song, and H. Gao, A new global best guided artificial bee colony algorithm with application in robot path planning, *Appl. Soft Comput.*, vol. 88, p. 106037, 2020.

[61] Z. Han, M. Chen, S. Shao, and Q. Wu, Improved artificial bee colony algorithm-based path planning of unmanned autonomous helicopter using multi-strategy evolutionary learning, *Aerosp. Sci. Technol.*, vol. 122, p. 107374, 2022.

[62] Y. Cui, W. Hu, and A. Rahmani, Fractional-order artificial

bee colony algorithm with application in robot path planning, *Eur. J. Oper. Res.*, vol. 306, no. 1, pp. 47–64, 2023.
[63] D. Lei and M. Liu, An artificial bee colony with division for distributed unrelated parallel machine scheduling with preventive maintenance, *Comput. Ind. Eng.*, vol. 141, p. 106320, 2020.
[64] D. Lei, Y. Yuan, and J. Cai, An improved artificial bee colony for multi-objective distributed unrelated parallel machine scheduling, *Int. J. Prod. Res.*, vol. 59, no. 17, pp. 5259–5271, 2021.
[65] V. Pandiri and A. Singh, A swarm intelligence approach for the colored traveling salesman problem, *Appl. Intell.*, vol. 48, no. 11, pp. 4412–4428, 2018.
[66] D. Karaboga and B. Gorkemli, Solving traveling salesman problem by using combinatorial artificial bee colony algorithms, *Int. J. Artif. Intell. Tools*, vol. 28, no. 1, p. 1950004, 2019.
[67] K. Guo and Q. Zhang, A discrete artificial bee colony algorithm for the reverse logistics location and routing problem, *Int. J. Info. Tech. Dec. Mak.*, vol. 16, no. 5, pp. 1339–1357, 2017.
[68] D. Lei, Z. Cui, and M. Li, A dynamical artificial bee colony for vehicle routing problem with drones, *Eng. Appl. Artif. Intell.*, vol. 107, p. 104510, 2022.
[69] D. Trachanatzi, M. Rigakis, M. Marinaki, Y. Marinakis, and N. Matsatsinis, Distance related: A procedure for applying directly artificial bee colony algorithm in routing problems, *Soft Comput.*, vol. 24, no. 12, pp. 9071–9089, 2020.
[70] V. F. Yu, P. Jodiawan, and A. Gunawan, An adaptive large neighborhood search for the green mixed fleet vehicle routing problem with realistic energy consumption and partial recharges, *Appl. Soft Comput.*, vol. 105, p. 107251, 2021.
[71] K. K. H. Ng, C. K. M. Lee, S. Z. Zhang, K. Wu, and W. Ho, A multiple colonies artificial bee colony algorithm for a capacitated vehicle routing problem and re-routing strategies under time-dependent traffic congestion, *Comput. Ind. Eng.*, vol. 109, pp. 151–168, 2017.
[72] Y. Guo, G. Chen, M. Jiang, D. Gong, and J. Liang, A knowledge guided transfer strategy for evolutionary dynamic multiobjective optimization, *IEEE Trans. Evol. Comput.*, doi: 10.1109/TEVC.2022.3222844.
[73] N. R. Sabar, A. Bhaskar, E. Chung, A. Turky, and A. Song, An adaptive memetic approach for heterogeneous vehicle routing problems with two-dimensional loading constraints, *Swarm Evol. Comput.*, vol. 58, p. 100730, 2020.
[74] Z. Guo, Y. Li, X. Jiang, and S. Gao, The electric vehicle routing problem with time windows using genetic algorithm, in *Proc. 2017 IEEE 2nd Advanced Information Technology, Electronic and Automation Control Conference* (*IAEAC*), Chongqing, China, 2017, pp. 635–639.
[75] K. -P. Wang, L. Huang, C. -G. Zhou, and W. Pang, Particle swarm optimization for traveling salesman problem, in *Proc. 2003 Int. Conf. Machine Learning and Cybernetics* (*IEEE Cat. No. 03EX693*), Xi'an, China, 2003, pp. 1583–1585.
[76] M. Mavrovouniotis, G. Ellinas, and M. Polycarpou, Ant colony optimization for the electric vehicle routing problem, in *Proc. 2018 IEEE Symp. Series on Computational Intelligence* (*SSCI*), Bangalore, India, 2018, pp. 1234–1241.
[77] K. Shao, K. Zhou, J. Qiu, and J. Zhao, ABC algorithm for VRP, in *Proc. 9th International Conference on Bio-Inspired Computing: Theories and Applications*, Wuhan, China, 2014, pp. 370–373.

**Yao Huang** received the BEng degree in automation from Nanjing University of Information Science and Technology Binjiang College and the MS degree in control engineering from Nanjing University of Information Science and Technology, Nanjing, China in 2017 and 2020, respectively. He is currently pursuing the PhD degree in mechanical engineering in China University of Mining and Technology (Beijing). His main research interests include multi-objective optimization, path planning, and vehicle scheduling.

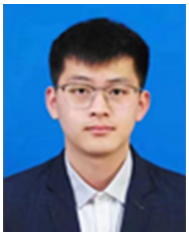

**Yizhe Zhang** received the BEng and MS degrees in mechanical engineering from Liaoning Technical University, Fuxin, China in 2017 and 2020, respectively. He is currently pursuing the PhD degree in mechanical engineering in China University of Mining and Technology (Beijing). His current research interests include intelligent mining equipment, mine unmanned driving, and intelligent optimal scheduling.

**Shirong Ge** received the BEng degree in coal mine mechanization from Heilongjiang University of Science and Technology, Heilongjiang, China in 1983, the MS and PhD degrees in mine mechanical engineering from China University of Mining and Technology, Xuzhou, China in 1986 and 1989, respectively. He is currently a professor at the School of Mechanical Electronic and Information Engineering, China University of Mining and Technology (Beijing), Beijing, China. His current research interests include intelligent mining equipment and friction reliability.

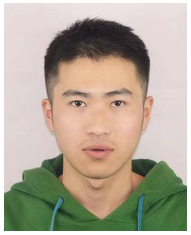

**Ersong Jiang** received the BEng degree in mechanical design, manufacturing, and automation from North China Institute of Science and Technology, Langfang, China in 2020. He is currently pursuing the MS degree in mechanical engineering in China University of Mining and Technology (Beijing). His main research interests include path planning and vehicle scheduling.

**Yinan Guo** received the BEng degree in automation and the PhD degree in control theory and control engineering from China University of Mining and Technology, Xuzhou, China in 1997 and 2003, respectively. She is currently a professor at the School of Mechanical Electronic and Information Engineering, China University of Mining and Technology (Beijing), Beijing, China. She has more than 90 publications. She is a member of IEEE. Her current research interests include computation intelligence in dynamic and uncertain optimization and its applications in scheduling, path planning, big data processing, and class imbalance learning and its applications in fault diagnosis.

**Shengxiang Yang** received the PhD degree from Northeastern University, Shenyang, China in 1999. He is a senior member of IEEE. He is currently a professor of computational intelligence and the deputy director of the Institute of Artificial Intelligence, School of Computer Science and Informatics, De Montfort University, Leicester, UK. He has over 360 publications with an H-index of 64 according to Google Scholar. His current research interests include evolutionary computation, swarm intelligence, artificial neural networks, data mining and data stream mining, and relevant real-world applications. He serves as an associate editor/editorial board member of a number of international journals, such as the *IEEE Transactions on Evolutionary Computation*, *IEEE Transactions on Cybernetics*, *Information Sciences*, and *CAAI Transactions on Intelligence Technology*.

**Bin Cheng** received the BEng degree in mechanical design, manufacturing, and automation from Shanghai University of Engineering Science, Shanghai, China in 2021. He is currently pursuing the MS degree in mechanical engineering at China University of Mining and Technology (Beijing). His main research interests include path planning and vehicle scheduling.